Homotrinuclear Lanthanide(III) Arrays: Assembly of and Conversion from Mononuclear and Dinuclear Units†

Ika A. Setyawati, Shuang Liu,‡ Steven J. Rettig, and Chris Orvig*

Medicinal Inorganic Chemistry Group, Department of Chemistry, University of British Columbia, 2036 Main Mall, Vancouver, BC V6T 1Z1, Canada

Received October 4, 1999

The reactions of potentially hexadentate H_2bbpen (*N*,*N*′-bis(2-hydroxybenzyl)-*N*,*N*′-bis(2-pyridylmethyl)-ethylenediamine, H_2L1), H_2(Cl)bbpen (*N*,*N*′-bis(5-chloro-2-hydroxybenzyl)-*N*,*N*′-bis(2-pyridylmethyl)ethylenediamine, H_2L2), and H_2(Br)bbpen (*N*,*N*′-bis(5-bromo-2-hydroxybenzyl)-*N*,*N*′-bis(2-pyridylmethyl)ethylenediamine, H_2L3) with Ln(III) ions in the presence of a base in methanol resulted in three types of complexes: neutral mononuclear ($[LnL(NO_3)]$), monocationic dinuclear ($[Ln_2L_2(NO_3)]^+$), and monocationic trinuclear ($[Ln_3L_2(X)_n(CH_3OH)]^+$), where X = bridging (CH_3COO^-) and bidentate ligands (NO_3^-, CH_3COO^-, ClO_4^-) and *n* is 4. The formation of a complex depends on the base (hydroxide or acetate) and the size of the respective Ln(III) ion. All complexes were characterized by infrared spectroscopy, mass spectrometry, and elemental analyses; in some cases, X-ray diffraction studies were also performed. The structures of the neutral mononuclear $[Yb(L1)(NO_3)]$, dinuclear $[Pr_2(L1)_2(NO_3)(H_2O)]NO_3\cdot CH_3OH$ and $[Gd_2(L1)_2(NO_3)]NO_3\cdot CH_3OH\cdot 3H_2O$, and trinuclear $[Gd_3(L3)_2(CH_3COO)_4(CH_3OH)]ClO_4\cdot 5CH_3OH$ and $[Sm_3(L1)_2(CH_3COO)_2(NO_3)_2(CH_3OH)]NO_3\cdot CH_3OH\cdot 3.65H_2O$ were solved by X-ray crystallography. The $[LnL(NO_3)]$ or $[Ln_2L_2(NO_3)]^+$ complexes could be converted to $[Ln_3L_2(X)_n(CH_3OH)]^+$ complexes by the addition of 1 equiv of a Ln(III) salt and 2−3 equiv of sodium acetate in methanol. The trinuclear complexes were found to be the most stable of the three types, which was evident from the presence of the intact monocationic high molecular weight parent peaks ($[Ln_3L_2(X)_n]^+$) in the mass spectra of all the trinuclear complexes and from the ease of conversion from the mononuclear or dinuclear to the trinuclear species. The incompatibility of the ligand denticity with the coordination requirements of the Ln(III) ions was proven to be a useful tool in the construction of multinuclear Ln(III) metal ion arrays.

Introduction

Much of the research on the chemistry of lanthanide(III) (Ln(III)) metal ions in recent years has focused on their potential uses in bioinorganic chemistry and materials science.[1−3] A concomitant growing interest has also been directed toward the design of polydentate chelating ligands capable of forming stable Ln(III) complexes for radiotherapy in nuclear medicine because of the rich array of isotopes available[4−7] and as contrast agents for magnetic resonance imaging (MRI).[8] Recent reviews of both applications are available in the September 1999 issue of *Chemical Reviews*.[9]

We have been exploring the chemistry of Ln(III) ions with multidentate ligands, particularly Schiff bases, amine phenolates, amine phosphinates, and amine pyridyl carboxylates.[10−12] In the process, a plethora of different coordination geometries around Ln(III) centers have been discovered, including two (encapsulated dimer and sandwich dimer) that contain dinuclear Ln(III) complexes with bridging phenolate oxygen atoms and geometries which can be controlled by appropriate ligand architecture (Chart 1). Compartmental Schiff bases,[13,14] including some acyclic examples,[14,15] have also been used to simultaneously incorporate two or more Ln(III) ions and a combination of Ln(III)−3d-metal ions; the resulting species also usually contain bridging phenolate oxygen atoms. The phenolate and alkoxo moieties of 2,6-bis[(dimethylamino)methyl]-4-methylphenol (bdmmp) and 1,3-bis(dimethylamino)-2-propanol (bdmapH), respectively, and the hydroxo group are also found as bridging

* To whom correspondence should be addressed. Tel.: 604-822-4449. Fax: 604-822-2847. E-mail: orvig@chem.ubc.ca.

† This paper is dedicated to our dear friend and sadly missed colleague Steven J. Rettig.

‡ Present address: Medical Imaging Division, DuPont Pharmaceuticals Co., 331 Treble Cove Rd., North Billerica, MA 01862.

(1) Evans, C. H. *Biochemistry of Lanthanides*; Plenum: New York, 1990; p 47.
(2) Spedding, F. H. In *Kirk-Othmer Encyclopedia of Chemical Technology*, 3rd ed.; Grayson, M., Eckroth, D., Eds.; Wiley: New York, 1982; Vol. 19, p 833.
(3) *Lanthanide Probes in Life, Chemical and Earth Sciences*; Bünzli, J.-C. G., Choppin, G. R., Eds.; Elsevier: Amsterdam, 1989.
(4) Order, S. E.; Klein, J. L.; Leicher, P. K.; Frinke, J.; Collo, C.; Carlo, D. J. *Int. J. Radiat. Oncol. Biol. Phys.* **1986**, *12*, 277.
(5) Cox, J. P. L.; Jakowski, K. J.; Kataky, R.; Beely, R. A.; Boyce, B. A.; Eaton, M. A. W.; Miller, K.; Millican, A. T.; Harrison, S.; Walker, C.; Parker, D. *J. Chem. Soc., Chem. Commun.* **1989**, 797.
(6) Norman, T. J.; Parker, D.; Royle, L.; Harrison, A.; Antoniw, P.; King, D. J. *J. Chem. Soc., Chem. Commun.* **1995**, 1877.
(7) Parker, D. *Chem. Br.* **1994**, *30*, 818.
(8) Lauffer, R. B. *Chem. Rev.* **1987**, *87*, 901.
(9) The September 1999 issue of *Chemical Reviews* is dedicated to medicinal inorganic chemistry topics.
(10) Caravan, P.; Lowe, M. P.; Read, P. W.; Rettig, S. J.; Yang, L.-W.; Orvig, C. *J. Alloys Compd.* **1997**, *249*, 49 and references therein.
(11) Caravan, P.; Mehrkhodavandi, P.; Orvig, C. *Inorg. Chem.* **1997**, *36*, 1316.
(12) Lowe, M. P.; Caravan, P.; Rettig, S. J.; Orvig, C. *Inorg. Chem.* **1998**, *37*, 1637.
(13) Guerriero, P.; Tamburini, S.; Vigato, P. A. *Coord. Chem. Rev.* **1995**, *139*, 17 and references therein.
(14) Aguiari, A.; Brianese, N.; Tamburini, S.; Vigato, P. A. *Inorg. Chim. Acta* **1995**, 233.
(15) Howell, R. C.; Spence, K. V. N.; Kahwa, I. A.; White, A. J. P.; Williams, D. J. *J. Chem. Soc., Dalton Trans.* **1996**, 961.

10.1021/ic991170j CCC: $19.00 © 2000 American Chemical Society
Published on Web 01/15/2000

Chart 1

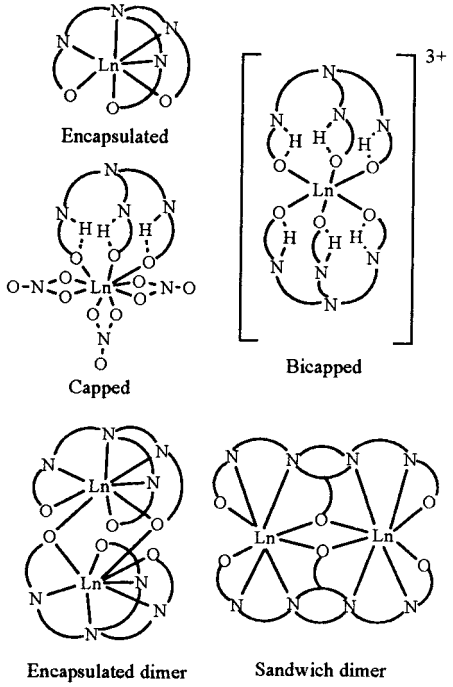

ligands in Ln(III)−3d-metal ion aggregates.[16,17] Ln(III) complexations with hexahomotrioxacalix[3]arene macrocylic ligands have been known to form dimers containing bridging aryloxide oxygen atoms as well.[18] Other examples of polynuclear Ln(III) complexes are those with bridging acetates[19,20] and with bridging trifluoroacetates.[17] In the development of MRI agents, some multinuclear Ln(III) complexes have been found. In the attempt to grow crystals of Gd(DO3A) (DO3A = 1,4,7-tris(carboxymethyl)-1,4,7,10-tetraazacyclododecane), Chang et al.[21] reported a trimeric $[\{Gd(DO3A)\}_3 \cdot Na_2CO_3] \cdot 17H_2O$ structure, in which three mononuclear Gd(DO3A) units were linked by one carbonate through two oxygen atoms bound to each Gd. Hegetschweiler and co-workers[22] discovered sandwich-type cage structures of trinuclear $[M_3(H_{-3}L)_2]^{3+}$ complexes [M = La, Gd; L = 1,3,5-triamino-1,3,5-trideoxy-*cis*-inositol (taci)] which contain three Ln(III) ions, two triply deprotonated taci ligands with bridging alkoxo groups, and chloride anions and/or water molecules in the coordination spheres. Other examples of multinuclear Ln(III) complexes of MRI interest were those with tripodal poly(iminocarboxylate) ligands in which carboxylate pendant arms formed bridges.[23]

The results with compartmental ligands,[13−15] with macrocylic hexahomotrioxacalix[3]arene ligands,[18] with the taci ligand,[22] with small ligand bridges[16,17,19,20] of other groups, and with multidentate ligands from our laboratory[10,12] suggested to us the construction of multinuclear lanthanide and mixed lanthanide−transition metal ion arrays. In another part of the project, the latter will be elaborated upon in the aggregation of and interaction among Ln(III) and 3d-metal ions.[24] In this contribution, the syntheses and characterizations of Ln(III) complexes containing deprotonated H_2bbpen (H_2L1), H_2(Cl)bbpen (H_2L2), and H_2(Br)bbpen (H_2L3) will be discussed.

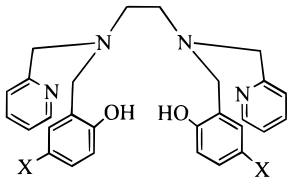

X = H, H_2bbpen (H_2L1)
= Cl, H_2Clbbpen (H_2L2)
= Br, H_2Brbbpen (H_2L3)

Three types of complexes were synthesized: neutral mononuclear ($[LnL(NO_3)]$), monocationic dinuclear ($[Ln_2L_2(NO_3)]^+$), and monocationic trinuclear ($[Ln_3L_2(X)_n(CH_3OH)]^+$) species, where X = bridging (CH_3COO^-) and bidentate ligands (NO_3^-, CH_3COO^-, ClO_4^-) and *n* is 4. The factors that control the types of complexes formed are the size of the Ln(III) ion and the base used in the reaction. Sodium hydroxide with small Ln(III) ions (Dy−Lu) resulted in $[LnL(NO_3)]$ complexes; meanwhile, the same base with larger Ln(III) ions (La−Gd) produced $[Ln_2L_2(NO_3)]^+$ complexes. Similar reactions in the presence of acetate, replacing hydroxide, resulted in the formation of $[Ln_3L_2(X)_n(CH_3OH)]^+$ complexes in which acetate anions and ligand phenolate oxygen atoms acted as bridges among three Ln(III) units. In a very simple one-step reaction, $[LnL(NO_3)]$ and $[Ln_2L_2(NO_3)]^+$ complexes (which are insoluble in methanol) can be converted to $[Ln_3L_2(X)_n(CH_3OH)]^+$ complexes, which are very soluble in methanol.

The coordination number of Ln(III) in these complexes varies from 7 to 9. The ligands reported herein (H_2L1−H_2L3) are potentially hexadentate and clearly do not satisfy the coordination number requirement of Ln(III) ions. The mismatch of ligand denticity with Ln(III) coordination numbers can be utilized specifically to create multinuclear species with or without additional small bridging ligands.

Experimental Section

Materials. Hydrated lanthanide salts, ethylenediamine, salicylaldehyde, sodium borohydride, 2-picolyl chloride hydrochloride, hexadecyltrimethylammonium bromide, and anhydrous sodium acetate were obtained from Aldrich or Alfa and were used without further purification. *N*,*N*′-Bis(salicylidene)etylenediamine (H_2salen),[25] *N*,*N*′-bis(2-hydroxybenzyl)ethylenediamine (H_2bben), *N*,*N*′-bis(2-hydroxybenzyl)-*N*,*N*′-bis(2-pyridylmethyl)ethylenediamine (H_2bbpen, H_2L1), *N*,*N*′-bis(5-chloro-2-hydroxybenzyl)-*N*,*N*′-bis(2-pyridylmethyl)ethylenediamine (H_2(Cl)bbpen, H_2L2), and *N*,*N*′-bis(5-bromo-2-hydroxybenzyl)-*N*,*N*′-bis(2-pyridylmethyl)ethylenediamine (H_2(Br)bbpen, H_2L3) were all prepared as described in the literature.[26]

Instrumentation. Mass spectra (Cs^+, LSIMS (liquid secondary ion mass spectrometry)) were obtained on a Kratos Concept II H32Q instrument with thioglycerol as the matrix. Infrared (IR) spectra were recorded as KBr disks in the range 4000−500 cm^{-1} on a Galaxy Series 5000 FTIR spectrometer. C, H, N, and Cl analyses were performed by Mr. Peter Borda of this department. Room-temperature magnetic susceptibilities of some lanthanide complexes were measured on a

(16) Chen, L.; Breeze, S. R.; Rousseau, R. J.; Wang, S.; Thompson, L. K. *Inorg. Chem.* **1995**, *34*, 454.
(17) Wang, S.; Pang, Z.; Smith, K. D. L.; Hua, Y.-S.; Deslippe, C.; Wagner, M. J. *Inorg. Chem.* **1995**, *34*, 908.
(18) Daitch, C. E.; Hampton, P. D.; Duesler, E. N.; Alam, T. M. *J. Am. Chem. Soc.* **1996**, *118*, 7769.
(19) Smith, P. H.; Ryan, R. R. *Acta Crystallogr., Sect. C* **1992**, *48*, 2127.
(20) Ouchi, A.; Suzuki, Y.; Ohki, Y.; Koizumi, Y. *Coord. Chem. Rev.* **1988**, *92*, 29.
(21) Chang, C. A.; Francesconi, L. C.; Malley, M. F.; Kumar, K.; Gougoutas, J. Z.; Tweedle, M. F. *Inorg. Chem.* **1993**, *32*, 3501.
(22) Hedinger, R.; Ghisletta, M.; Hegetschweiler, K.; Tóth, E.; Merbach, A. E.; Sessoli, R.; Gatteschi, D.; Gramlich, V. *Inorg. Chem.* **1998**, *37*, 6698.
(23) Blake, A. J.; Doble, D. M. J.; Li, W.-S.; Schroder, M. *J. Chem. Soc., Dalton Trans.* **1997**, 3655.
(24) Xu, Z.; Read, P. W.; Hibbs, D. E.; Hursthouse, M. B.; Abdul Malik, K. M.; Patrick, B. O.; Rettig, S. J.; Seid, M.; Summers, D. A.; Pink, M.; Thompson, R. C.; Orvig, C. *Inorg. Chem.* **2000**, *39*, 508.
(25) Diehl, D.; Hach, C. C. *Inorg. Synth.* **1950**, *3*, 196.
(26) Wong, E.; Liu, S.; Rettig, S. J. Orvig, C. *Inorg. Chem.* **1995**, *34*, 3057−3064.

Table 1. Infrared Spectral Data for Nitrates, Acetates, and Bridging Phenolates (cm^{-1}; KBr Disk) in the Lanthanide Complexes[a]

complex	$\nu_{NO_3^-}$ free (s)	$\nu_{NO_3^-}$ bidentate (s)	$\delta_{C-O(phenolate\ bridge)}$ (s)	ν_{COO^-} bridging (m)	ν_{COO^-} bidentate (m)
$[Dy(L1)(NO_3)]$		1480,[b] 1298			
$[Er(L1)(NO_3)]$		1479,[b] 1300			
$[Yb(L1)(NO_3)]\cdot 0.5H_2O$		1481,[b] 1300			
$[Lu(L1)(NO_3)]$		1481,[b] 1302			
$[La_2(L1)_2(NO_3)]NO_3\cdot H_2O$	1384	1479,[b] 1288	1260		
$[Pr_2(L1)_2(NO_3)]NO_3\cdot 3H_2O$	1385	1480,[b] 1287	1260		
$[Sm_2(L1)_2(NO_3)]NO_3\cdot 2H_2O$	1383	1480,[b] 1289	1260		
$[Gd_2(L1)_2(NO_3)]NO_3\cdot 3H_2O$	1384	1481,[b] 1290	1260		
$[Pr_3(L1)_2(CH_3COO)_2(NO_3)_2(CH_3OH)]NO_3\cdot 5H_2O$	1384	1481,[b] 1290	1258	1566, 1414	
$[Sm_3(L1)_2(CH_3COO)_2(NO_3)_2(CH_3OH)]NO_3\cdot CH_3OH\cdot 5H_2O$	1385	1482,[b] 1292	1260	1564, 1413	
$[Gd_3(L1)_2(CH_3COO)_2(NO_3)_2(CH_3OH)]NO_3\cdot 2H_2O$	1385	1483,[b] 1310	1258	1566, 1412	
$[Lu_3(L1)_2(CH_3COO)_3(NO_3)(CH_3OH)]NO_3\cdot 2H_2O$	1384	1485[b]	1257	1564, 1412	1552, 1451
$[Gd_3(L1)_2(CH_3COO)_2(NO_3)_2(CH_3OH)]PF_6\cdot H_2O$	844 (br) (PF_6^-)	1484,[b] 1296	1259	1564, 1412	
$[Gd_3(L3)_2(CH_3COO)_4(CH_3OH)]ClO_4\cdot H_2O$	1100 (br) (ClO_4^-)		1265	1563, 1413	1551, 1450
$[Ho_3(L2)_2(CH_3COO)_3(ClO_4)(CH_3OH)]ClO_4\cdot H_2O$	1092 (br) (ClO_4^-)		1263	1560, 1416	1532, 1451
$[Yb_3(L1)_2(CH_3COO)_3(ClO_4)(CH_3OH)]ClO_4$	1097 (br) (ClO_4^-)		1257	1564, 1414	1547, 1446

[a] s = strong, m = medium, br = broad. [b] Overlapping with $\nu_{C=C}$ of the ligand. For all complexes, $\nu_{C=C}$ and $\nu_{C=N}$ are present around 1600 cm^{-1}.

Table 2. LSIMS Data for the Lanthanide Complexes (+ Mode)

complex	$[Ln(L)]^+$ [a]	$[Ln_2(L)_2(NO_3)]^+$	$[Ln_2(L)(OAc)_x(NO_3)_y(ClO_4)_z]^+$	$[Ln_3(L)_2(OAc)_x(NO_3)_y(ClO_4)_z]^+$
$[Dy(L1)(NO_3)]$	616			
$[Er(L1)(NO_3)]$	620			
$[Yb(L1)(NO_3)]\cdot 0.5H_2O$	626			
$[Lu(L1)(NO_3)]$	627			
$[La_2(L1)_2(NO_3)]NO_3\cdot H_2O$	591	1244		
$[Pr_2(L1)_2(NO_3)]NO_3\cdot 3H_2O$	593	1248		
$[Sm_2(L1)_2(NO_3)]NO_3\cdot 2H_2O$	604			
$[Gd_2(L1)_2(NO_3)]NO_3\cdot 3H_2O$	610	1282		
$[Pr_3(L1)_2(CH_3COO)_2(NO_3)_2(CH_3OH)]NO_3\cdot 5H_2O$	593		914, (2, 1, 0)[b]	1569, (2, 2, 0)
$[Sm_3(L1)_2(CH_3COO)_2(NO_3)_2(CH_3OH)]NO_3\cdot CH_3OH\cdot 5H_2O$	604		933, (2, 1, 0)	1599, (2, 2, 0)
$[Gd_3(L1)_2(CH_3COO)_2(NO_3)_2(CH_3OH)]NO_3\cdot 2H_2O$	610		948, (2, 1, 0)	1619, (2, 2, 0)
$[Gd_3(L1)_2(CH_3COO)_2(NO_3)_2(CH_3OH)]PF_6\cdot H_2O$	610			
$[Gd_3(L3)_2(CH_3COO)_4(CH_3OH)]ClO_4\cdot H_2O$	768			1929, (4, 0, 0)
$[Ho_3(L2)_2(CH_3COO)_3(ClO_4)(CH_3OH)]ClO_4\cdot H_2O$	685			
$[Yb_3(L1)_2(CH_3COO)_3(ClO_4)(CH_3OH)]ClO_4$	626		975, (3, 0, 0)	
$[Lu_3(L1)_2(CH_3COO)_3(NO_3)(CH_3OH)]NO_3\cdot 2H_2O$	627		979, (3, 0, 0)	1668, (3, 1, 0)

[a] For all complexes, $[Ln(L - \text{one phenol arm})]^+$ ($[Ln(L)]^+ - 106$) fragments are always present. [b] The numbers inside all parentheses are *x*, *y*, *z* values, respectively.

Johnson Matthey magnetic susceptibility balance using $Hg[Co(NCS)_4]$ as the susceptibility standard.

Syntheses of the Metal Complexes. The preparations of mononuclear ($[LnL(NO_3)]$) and dinuclear ($[Ln_2L_2(NO_3)]NO_3$) complexes were similar; thus, detailed procedures are given for representative examples, and all compounds prepared, along with their characterization data, are listed in Tables 1−3.

Caution! *It should be noted that perchlorate salts of metal complexes are potentially explosive and should be handled with care.*

$[Ln(L1)(NO_3)]\cdot mH_2O$ (Ln = Dy). To a methanolic solution of H_2-L1 (0.093 g, 0.2 mmol) and 50 μL of 8 M NaOH (0.4 mmol) was added a methanolic solution of $Dy(NO_3)_3\cdot 5H_2O$ (0.087 g, 0.2 mmol). The mixture was stirred at room temperature for 1 h. The resulting precipitate was collected by vacuum filtration and dried in air; yield 103 mg (75%). Yields for the other mononuclear complexes: Er, 88%; Yb, 81%; Lu, 91%.

$[Ln_2(L1)_2(NO_3)]NO_3\cdot mH_2O$. These complexes were prepared similarly to the mononuclear Dy−Lu complexes. Yields for the dinuclear complexes: La, 63%; Pr, 88%; Sm, 64%; Gd, 86%.

General Preparative Method for the Trinuclear Complexes ($[Ln_3L_2(X)_n(CH_3OH)]Y$; Y = Counteranion) (Details Provided in Table 4). To a suspension of 0.2 mmol of H_2L and 0.5 mmol of anhydrous sodium acetate ($NaCH_3COO$) in 10 mL of methanol was added 0.2 mmol of lanthanide salt. The mixture was stirred for 1 h at room temperature, after which it was filtered and, in some cases, a counteranion salt was added to the filtrate. The filtrate was left at room temperature for slow evaporation or was placed in a refrigerator. The product was collected by vacuum filtration and dried in air. Suitable crystals of the trinuclear complexes (Ln = Sm, Gd) were obtained from slow evaporation at room temperature and recrystallization from methanol, respectively, and were used in X-ray diffraction studies (vide infra).

General Preparative Method for the Conversion of $[LnL(NO_3)]$ or $[Ln_2L_2(NO_3)]NO_3$ to $[Ln_3L_2(X)_n(CH_3OH)]Y$ Complexes (Scheme 1). To a suspension of $[Gd_2(L1)_2(NO_3)]NO_3\cdot 3H_2O$ (420 mg, 0.3 mmol) in methanol were added $Gd(NO_3)_3\cdot 6H_2O$ (136 mg, 0.3 mmol) and anhydrous sodium acetate (55 mg, 0.6 mmol); the initial solution was cloudy white. While being stirred for 1 h at room temperature, the suspension became clear. The solution was filtered, and the filtrate was left at room temperature for slow evaporation. The white precipitate (304 mg, 58% yield) was collected via vacuum filtration and dried in air. Similar procedures were followed for Pr and Lu; yields were 25% and 20%, respectively. IR spectra, elemental analyses, and mass spectra showed that the resulting products have the general formula $[Ln_3(L1)_2(CH_3COO)_2(NO_3)_2(CH_3OH)]NO_3\cdot mH_2O$. The same complexes can also be obtained from the reaction of $[Gd_2(L1)_2(NO_3)]NO_3$ and $Gd(CH_3COO)_3$ or from the reaction of $[Gd_2(L1)_2(NO_3)]NO_3$, $GdCl_3\cdot 6H_2O$, and anhydrous sodium acetate.

Table 3. Analytical Data [Calcd (Found)] and Room-Temperature Magnetic Moments for the Lanthanide Complexes

complex	% C	% H	% N	μ_{eff}/Ln^{III}, μB
$[Dy(L1)(NO_3)]$	49.67 (49.58)	4.17 (4.14)	10.34 (10.09)	10.43
$[Er(L1)(NO_3)]$	49.33 (49.14)	4.14 (4.21)	10.27 (9.98)	
$[Yb(L1)(NO_3)]\cdot 0.5H_2O$	48.28 (48.16)	4.20 (4.20)	10.05 (9.87)	4.48
$[Lu(L1)(NO_3)]$	48.77 (48.99)	4.09 (4.07)	10.16 (9.85)	diamag
$[La_2(L1)_2(NO_3)]NO_3\cdot H_2O$	50.77 (50.69)	4.41 (4.53)	10.57 (10.43)	diamag
$[Pr_2(L1)_2(NO_3)]NO_3\cdot 3H_2O$	49.28 (49.28)	4.58 (4.55)	(10.02)	3.35
$[Sm_2(L1)_2(NO_3)]NO_3\cdot 2H_2O$	49.24 (49.43)	4.43 (4.30)	10.25 (9.96)	
$[Gd_2(L1)_2(NO_3)]NO_3\cdot 3H_2O$	48.12 (48.13)	4.47 (4.16)	10.02 (9.92)	8.26
$[Pr_3(L1)_2(CH_3COO)_2(NO_3)_2(CH_3OH)]NO_3\cdot 5H_2O$	41.77 (41.75)	4.37 (4.40)	8.78 (8.68)	
$[Sm_3(L1)_2(CH_3COO)_2(NO_3)_2(CH_3OH)]NO_3\cdot CH_3OH\cdot 5H_2O$	41.04 (40.67)	4.44 (4.13)	8.49 (8.40)	
$[Gd_3(L1)_2(CH_3COO)_2(NO_3)_2(CH_3OH)]NO_3\cdot 2H_2O$	41.89 (41.97)	4.03 (3.79)	8.81 (8.91)	8.11
$[Gd_3(L1)_2(CH_3COO)_2(NO_3)_2(CH_3OH)]PF_6\cdot H_2O$	40.39 (40.29)	3.78 (3.40)	7.72 (7.45)	
$[Gd_3(L3)_2(CH_3COO)_4(CH_3OH)]ClO_4\cdot H_2O$	37.57 (37.49)	3.40 (3.48)	5.39 (5.32)	7.91
$[Ho_3(L2)_2(CH_3COO)_3(ClO_4)(CH_3OH)]ClO_4\cdot H_2O$	38.53 (38.37)	3.44 (3.15)	5.71 (5.60)	
$[Yb_3(L1)_2(CH_3COO)_3(ClO_4)(CH_3OH)]ClO_4$	41.30 (41.32)	3.80 (3.63)	6.12 (6.06) 3.87 (4.15) (Cl)	
$[Lu_3(L1)_2(CH_3COO)_3(NO_3)(CH_3OH)]NO_3\cdot 2H_2O$	42.06 (42.04)	4.09 (3.90)	7.78 (7.70)	diamag

Table 4. Preparative Details for the Trinuclear ($[Ln_3L_2(X)_n(CH_3OH)]Y$) Complexes

Ln(III) salt starting material	ligand	counteranion salt added	product	yield, %
$Pr(NO_3)_3\cdot 6H_2O$	H_2L1	none	$[Pr_3(L1)_2(CH_3COO)_2(NO_3)_2(CH_3OH)]NO_3\cdot 5H_2O$	25
$Sm(NO_3)_3\cdot 6H_2O$	H_2L1	none	$[Sm_3(L1)_2(CH_3COO)_2(NO_3)_2(CH_3OH)]NO_3\cdot CH_3OH\cdot 5H_2O$	35
$Gd(NO_3)_3\cdot 6H_2O$	H_2L1	none	$[Gd_3(L1)_2(CH_3COO)_2(NO_3)_2(CH_3OH)]NO_3\cdot 2H_2O$	29
$Gd(NO_3)_3\cdot 6H_2O$	H_2L1	$NaPF_6$	$[Gd_3(L1)_2(CH_3COO)_2(NO_3)_2(CH_3OH)]PF_6\cdot H_2O$	39
$GdCl_3\cdot 6H_2O$	H_2L3	$NaClO_4$	$[Gd_3(L3)_2(CH_3COO)_4(CH_3OH)]ClO_4\cdot H_2O$	48[a]
$Ho(ClO_4)_3\cdot 6H_2O$	H_2L2	none	$[Ho_3(L2)_2(CH_3COO)_3(ClO_4)(CH_3OH)]ClO_4\cdot H_2O$	73
$YbCl_3\cdot 6H_2O$	H_2L1	$NaClO_4$	$[Yb_3(L1)_2(CH_3COO)_3(ClO_4)(CH_3OH)]ClO_4$	25
$Lu(NO_3)_3\cdot 6H_2O$	H_2L1	none	$[Lu_3(L1)_2(CH_3COO)_3(NO_3)(CH_3OH)]NO_3\cdot 2H_2O$	17[a]

[a] Product after recrystallization from hot methanol.

Scheme 1

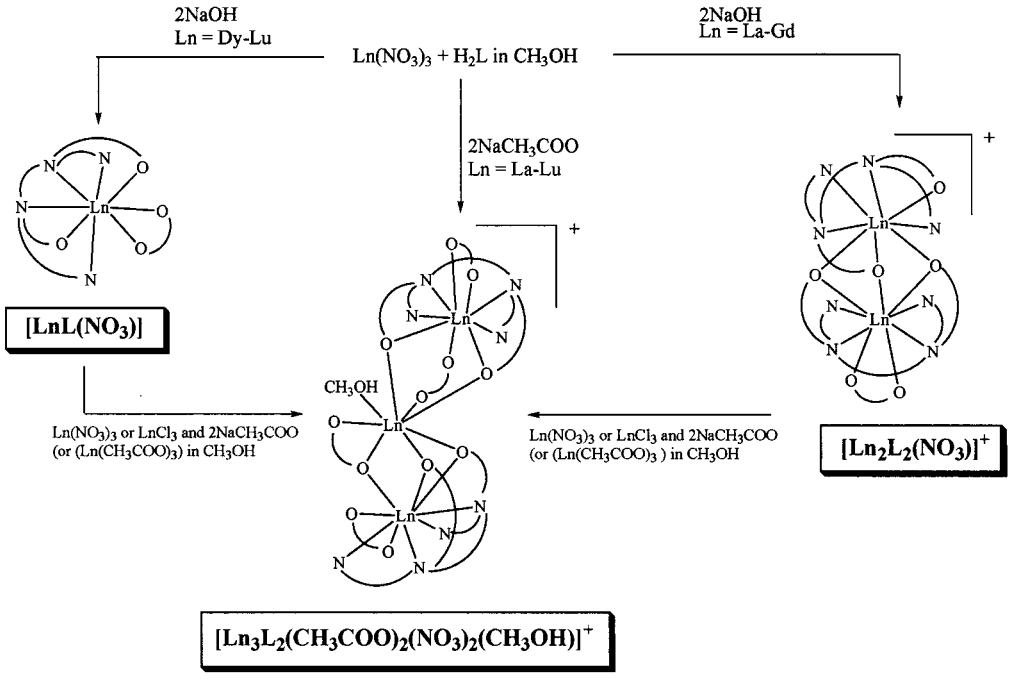

All complexes were characterized by IR spectroscopy (Table 1), mass spectrometry (Table 2), and elemental analyses (Table 3); in some cases, X-ray crystallography was also employed.

X-ray Crystallographic Analyses. Selected crystallographic data appear in Table 5. The final unit-cell parameters were based on 9544 reflections for $[Yb(L1)(NO_3)]$, 18 422 reflections for $[Pr_2(L1)_2(NO_3)(H_2O)]NO_3\cdot CH_3OH$, 32 835 reflections for $[Gd_2(L1)_2(NO_3)]NO_3\cdot CH_3OH\cdot 3H_2O$, 25 682 reflections for $[Gd_3(L3)_2(CH_3COO)_4(CH_3OH)]ClO_4\cdot 5CH_3OH$, and 45 418 reflections for $[Sm_3(L1)_2(CH_3COO)_2(NO_3)_2(CH_3OH)]NO_3\cdot CH_3OH\cdot 3.65H_2O$ with a maximum 2θ value of 60.1°. The data were processed[27] and corrected for Lorentz and polarization effects.

All structures were solved by heavy-atom Patterson methods and expanded using Fourier techniques. The non-hydrogen atoms were refined anisotropically, and the hydrogen atoms were fixed in calculated positions with C−H = 0.98 Å (for all complexes) and O−H = 0.95 Å

(27) *teXsan*: *Crystal Structure Analysis Package*; Molecular Structure Corp.: The Woodlands, TX, 1992.

Table 5. Selected Crystallographic Data for the Mononuclear, Dinuclear, and Trinuclear Ln(III) Complexes[a]

complex	[Yb(L1)(NO_3)]	[Pr_2(L1)$_2$(NO_3)(H_2O)]-NO_3·CH_3OH	[Gd_2(L1)$_2$(NO_3)]-NO_3·CH_3OH·3H_2O	[Gd_3(L3)$_2$(CH_3COO)$_4$-(CH_3OH)]ClO_4·5CH_3OH	[Sm_3(L1)$_2$(CH_3COO)$_2$(NO_3)$_2$-(CH_3OH)]NO_3·CH_3OH·3.65H_2O
empirical formula	$C_{28}H_{28}N_5O_5Yb$	$C_{57}H_{62}N_{10}O_{12}Pr_2$	$C_{57}H_{66}Gd_2N_{10}O_{14}$	$C_{70}H_{88}Br_4ClGd_3N_8O_{22}$	$C_{62}H_{77.30}N_{11}O_{22.65}Sm_3$
fw	687.60	1360.99	1429.71	2220.32	1790.25
cryst syst	orthorhombic	Triclinic	monoclinic	triclinic	monoclinic
space group	$C222_1$	$P\bar{1}$	$P2_1/n$	$P\bar{1}$	$P2_1/c$
a, Å	8.5562(10)	10.8171(7)	12.9850(7)	13.7301(9)	15.2433(4)
b, Å	18.1568(5)	13.242(2)	21.5181(15)	17.559(2)	22.8831(8)
c, Å	16.9577(6)	21.329(2)	22.1460(2)	18.4879(8)	20.96500(10)
α, deg		74.189(3)		103.8890(4)	
β, deg		83.5611(13)	106.9883(2)	92.6668(7)	99.7225(2)
γ, deg		73.9577(12)		110.268(2)	
V, Å^3	2634.4(2)	2822.8(4)	5917.9(4)	4017.5(5)	7207.9(2)
Z	4	2	4	2	4
ρ_{calc}, g/cm^3	1.734	1.601	1.605	1.835	1.650
μ, cm^{-1}	35.99	17.72	23.01	45.58	24.98
transm factor	0.7110−1.0000	0.6880−1.0000	0.6275−1.0000	0.6865−1.0000	0.8315−1.0000
R^b	0.032	0.026	0.037	0.052	0.042
$R_w{}^c$	0.030	0.024	0.029	0.054	0.040

[a] All data were collected at −93 °C using Mo Kα radiation (λ = 0.710 69). [b] $R = \sum||F_o| - |F_c||/\sum|F_o|$. [c] $R_w = [\sum w(|F_o| - |F_c|)^2/\sum w|F_o|^2]^{1/2}$.

Table 6. Selected Bond Lengths (Å) and Bond Angles (deg) in [Yb(L1)(NO_3)]

Yb(1)−O(1)	2.163(4)	Yb(1)−N(1)	2.504(4)
Yb(1)−O(2)	2.432(4)	Yb(1)−N(2)	2.508(4)
O(1)−Yb(1)−O(1*)[a]	156.3(2)	O(2)−Yb(1)−N(1)	141.15(14)
O(1)−Yb(1)−O(2)	128.19(14)	O(2)−Yb(1)−N(1*)	132.40(14)
O(1)−Yb(1)−O(2*)	75.49(14)	O(2)−Yb(1)−N(2)	79.17(15)
O(1)−Yb(1)−N(1)	77.65(14)	O(2)−Yb(1)−N(2*)	78.93(15)
O(1)−Yb(1)−N(1*)	83.11(14)	N(1)−Yb(1)−N(1*)	71.4(2)
O(1)−Yb(1)−N(2)	98.78(15)	N(1)−Yb(1)−N(2)	67.26(15)
O(1)−Yb(1)−N(2*)	86.25(14)	N(1)−Yb(1)−N(2*)	137.01(15)
O(2)−Yb(1)−O(2*)	53.1(2)	N(2)−Yb(1)−N(2*)	155.5(2)

[a] Asterisks indicate the symmetry operation 1 − *x*, *y*, $^1/_2$ − *z*.

Table 7. Selected Bond Lengths (Å) and Bond Angles (deg) in the Cation of [Pr_2(L1)$_2$(NO_3)(H_2O)]NO_3·CH_3OH

Pr(1)−O(1)	2.309(2)	Pr(2)−O(3)	2.377(2)
Pr(1)−O(2)	2.400(2)	Pr(2)−O(4)	2.448(2)
Pr(1)−O(3)	2.426(2)	Pr(2)−O(5)	2.588(2)
Pr(1)−O(4)	2.483(2)	Pr(2)−O(6)	2.588(2)
Pr(1)−N(1)	2.720(2)	Pr(2)−O(8)	2.448(2)
Pr(1)−N(2)	2.796(2)	Pr(2)−N(5)	2.712(2)
Pr(1)−N(3)	2.690(2)	Pr(2)−N(6)	2.717(3)
Pr(1)−N(4)	2.717(2)	Pr(2)−N(7)	2.643(2)
		Pr(2)−N(8)	2.652(3)
O(1)−Pr(1)−O(2)	165.92(7)	O(3)−Pr(2)−N(5)	72.29(6)
O(1)−Pr(1)−O(3)	93.70(6)	O(3)−Pr(2)−N(6)	104.51(7)
O(1)−Pr(1)−O(4)	80.10(7)	O(3)−Pr(2)−N(7)	75.79(7)
O(1)−Pr(1)−N(1)	70.39(7)	O(3)−Pr(2)−N(8)	149.30(6)
O(1)−Pr(1)−N(2)	120.70(7)	O(4)−Pr(2)−O(5)	130.43(6)
O(1)−Pr(1)−N(3)	104.29(7)	O(4)−Pr(2)−O(6)	146.06(7)
O(1)−Pr(1)−N(4)	74.47(7)	O(4)−Pr(2)−O(8)	74.37(6)
O(2)−Pr(1)−O(3)	78.54(6)	O(4)−Pr(2)−N(5)	115.14(7)
O(2)−Pr(1)−O(4)	86.06(7)	O(4)−Pr(2)−N(6)	74.32(6)
O(2)−Pr(1)−N(1)	120.05(6)	O(4)−Pr(2)−N(7)	141.83(7)
O(2)−Pr(1)−N(2)	73.35(7)	O(4)−Pr(2)−N(8)	80.42(7)
O(2)−Pr(1)−N(3)	75.66(7)	O(5)−Pr(2)−O(6)	49.44(7)
O(2)−Pr(1)−N(4)	115.06(7)	O(5)−Pr(2)−O(8)	71.39(7)
O(3) −Pr(1)−O(4)	67.60(6)	O(5)−Pr(2)−N(5)	113.89(6)
O(3)−Pr(1)−N(1)	157.88(7)	O(5)−Pr(2)−N(6)	119.40(7)
O(3)−Pr(1)−N(2)	113.29(6)	O(5)−Pr(2)−N(7)	68.63(7)
O(3)−Pr(1)−N(3)	139.94(7)	O(5)−Pr(2)−N(8)	68.04(7)
O(3)−Pr(1)−N(4)	79.96(6)	O(6)−Pr(2)−O(8)	120.74(7)
O(4)−Pr(1)−N(1)	121.97(6)	O(6)−Pr(2)−N(5)	72.73(7)
O(4)−Pr(1)−N(2)	158.36(7)	O(6)−Pr(2)−N(6)	79.47(7)
O(4)−Pr(1)−N(3)	80.46(6)	O(6)−Pr(2)−N(7)	72.09(7)
O(4)−Pr(1)−N(4)	137.00(6)	O(6)−Pr(2)−N(8)	68.75(7)
N(1)−Pr(1)−N(2)	65.91(7)	O(8)−Pr(2)−N(5)	142.67(7)
N(1)−Pr(1)−N(3)	61.25(7)	O(8)−Pr(2)−N(6)	144.54(6)
N(1)−Pr(1)−N(4)	80.96(7)	O(8)−Pr(2)−N(7)	85.28(7)
N(2)−Pr(1)−N(3)	87.91(7)	O(8)−Pr(2)−N(8)	94.72(7)
N(2)−Pr(1)−N(4)	61.02(7)	N(5)−Pr(2)−N(6)	67.75(7)
N(3)−Pr(1)−N(4)	139.08(7)	N(5)−Pr(2)−N(7)	65.04(7)
O(3)−Pr(2)−O(4)	68.93(6)	N(5)−Pr(2)−N(8)	122.00(7)
O(3)−Pr(2)−O(5)	134.90(7)	N(6)−Pr(2)−N(7)	130.08(7)
O(3)−Pr(2)−O(6)	139.89(6)	N(6)−Pr(2)−N(8)	63.93(8)
O(3)−Pr(2)−O(8)	79.08(7)	N(7)−Pr(2)−N(8)	134.12(8)
Pr(1)−O(3)−Pr(2)	113.71(7)	Pr(1)−O(4)−Pr(2)	109.31(7)

(for [Pr_2(L1)$_2$(NO_3)(H_2O)]NO_3·CH_3OH; 0.90 Å for both dinuclear and trinuclear Gd complexes). In the structure of [Sm_3(L1)$_2$(CH_3COO)$_2$-(NO_3)$_2$(CH_3OH)]NO_3·CH_3OH·3.65H_2O, two water molecules are ordered and the remaining 1.65 waters are distributed over five sites with site occupancies in the range 0.25−0.55. The partial O atoms were refined isotropically, and the remaining non-hydrogen atoms were refined anisotropically. Hydrogen atoms associated with the methanol and the ordered water molecules were fixed in difference map positions but were not refined. Hydrogen atoms associated with the disordered water were not included in the model. Neutral-atom scattering factors for all atoms and anomalous dispersion corrections for the non-hydrogen atoms were taken from the refs 28 and 29. Selected bond lengths and bond angles appear in Tables 6−10. Complete tables of crystallographic data, atomic coordinates and equivalent isotropic thermal parameters, hydrogen atom parameters, anisotropic thermal parameters, bond lengths, bond angles, torsion angles, intermolecular contacts, and least-squares planes are included as Supporting Information.

Results and Discussion

The complexations of $L1^{2-}$ ($bbpen^{2-}$), $L2^{2-}$ ($(Cl)bbpen^{2-}$), and $L3^{2-}$ ($(Br)bbpen^{2-}$) with lanthanide(III) (Ln(III)) ions result in three types of complexes depending on the base used in the reactions and on the size of Ln(III) (see Scheme 1). When 2 equiv of sodium hydroxide (NaOH) was used as a base with 1 equiv each of Ln(III) salt and ligand, smaller Ln(III) ions (Dy−Lu) formed neutral mononuclear complexes ([LnL(NO_3)]) containing one Ln(III), one ligand, and one bidentate nitrate in their coordination spheres. When similar reactions were performed with larger Ln(III) ions (La−Gd), monocationic dinuclear complexes ($[Ln_2L_2(NO_3)]^+$) were produced. These contained two Ln(III) ions, two L^{2-} ligands with bridging phenolate oxygen atoms, and one bidentate nitrate. Some complexes contained water molecules in their coordination

(28) *International Tables for X-ray Crystallography*; Kynoch Press: Birmingham, U.K., 1974; Vol. IV, pp 99−102.
(29) *International Tables for Crystallography*; Kluwer Academic Publishers: Boston, MA, 1992; Vol. C, pp 200−206.

Table 8. Selected Bond Lengths (Å) and Bond Angles (deg) in the Cation of $[Gd_2(L1)_2(NO_3)]NO_3 \cdot CH_3OH \cdot 3H_2O$

Gd(1)−O(1)	2.230(3)	Gd(2)−O(2)	2.336(3)
Gd(1)−O(2)	2.409(3)	Gd(2)−O(3)	2.361(3)
Gd(1)−O(3)	2.524(3)	Gd(2)−O(4)	2.467(3)
Gd(1)−O(4)	2.377(3)	Gd(2)−O(5)	2.481(3)
Gd(1)−N(1)	2.728(3)	Gd(2)−O(6)	2.507(3)
Gd(1)−N(2)	2.665(4)	Gd(2)−N(5)	2.586(3)
Gd(1)−N(3)	2.501(3)	Gd(2)−N(6)	2.697(4)
Gd(1)−N(4)	2.613(4)	Gd(2)−N(7)	2.654(4)
		Gd(2)−N(8)	2.647(4)
O(1)−Gd(1)−O(2)	142.16(11)	O(2)−Gd(2)−N(5)	153.16(11)
O(1)−Gd(1)−O(3)	85.07(10)	O(2)−Gd(2)−N(6)	131.99(12)
O(1)−Gd(1)−O(4)	123.91(10)	O(2)−Gd(2)−N(7)	99.30(10)
O(1)−Gd(1)−N(1)	74.06(11)	O(2)−Gd(2)−N(8)	84.85(11)
O(1)−Gd(1)−N(2)	136.18(11)	O(3)−Gd(2)−O(4)	66.45(10)
O(1)−Gd(1)−N(3)	78.38(11)	O(3)−Gd(2)−O(5)	139.22(11)
O(1)−Gd(1)−N(4)	85.25(12)	O(3)−Gd(2)−O(6)	122.31(10)
O(2)−Gd(1)−O(3)	69.37(9)	O(3)−Gd(2)−N(5)	80.66(11)
O(2)−Gd(1)−O(4)	70.59(9)	O(3)−Gd(2)−N(6)	118.50(11)
O(2)−Gd(1)−N(1)	116.16(10)	O(3)−Gd(2)−N(7)	71.67(11)
O(2)−Gd(1)−N(2)	75.81(11)	O(3)−Gd(2)−N(8)	151.45(11)
O(2)−Gd(1)−N(3)	74.79(11)	O(4)−Gd(2)−O(5)	148.95(10)
O(2)−Gd(1)−N(4)	132.33(11)	O(4)−Gd(2)−O(6)	139.50(9)
O(3)−Gd(1)−O(4)	65.28(10)	O(4)−Gd(2)−N(5)	105.92(10)
O(3)−Gd(1)−N(1)	150.48(10)	O(4)−Gd(2)−N(6)	73.59(11)
O(3)−Gd(1)−N(2)	138.37(10)	O(4)−Gd(2)−N(7)	138.10(11)
O(3)−Gd(1)−N(3)	91.01(11)	O(4)−Gd(2)−N(8)	89.07(11)
O(3)−Gd(1)−N(4)	126.64(10)	O(5)−Gd(2)−O(6)	51.88(9)
O(4)−Gd(1)−N(1)	144.12(11)	O(5)−Gd(2)−N(5)	70.92(11)
O(4)−Gd(1)−N(2)	82.31(10)	O(5)−Gd(2)−N(6)	76.99(11)
O(4)−Gd(1)−N(3)	143.11(11)	O(5)−Gd(2)−N(7)	70.09(11)
O(4)−Gd(1)−N(4)	77.73(10)	O(5)−Gd(2)−N(8)	68.99(12)
N(1)−Gd(1)−N(2)	66.91(11)	O(6)−Gd(2)−N(5)	114.44(11)
N(1)−Gd(1)−N(3)	64.81(11)	O(6)−Gd(2)−N(6)	118.60(11)
N(1)−Gd(1)−N(4)	72.99(10)	O(6)−Gd(2)−N(7)	67.31(11)
N(2)−Gd(1)−N(3)	101.37(11)	O(6)−Gd(2)−N(8)	67.26(11)
N(2)−Gd(1)−N(4)	65.25(11)	N(5)−Gd(2)−N(6)	67.53(12)
N(3)−Gd(1)−N(4)	137.43(11)	N(5)−Gd(2)−N(7)	65.10(11)
O(2)−Gd(2)−O(3)	73.47(10)	N(5)−Gd(2)−N(8)	121.95(11)
O(2)−Gd(2)−O(4)	70.26(9)	N(6)−Gd(2)−N(7)	128.70(11)
O(2)−Gd(2)−O(5)	126.3(29)	N(6)−Gd(2)−N(8)	63.87(11)
O(2)−Gd(2)−O(6)	75.10(10)	N(7)−Gd(2)−N(8)	131.44(12)
Gd(1)−O(2)−Gd(2)	100.03(10)	Gd(1)−O(4)−Gd(2)	97.28(10)
Gd(1)−O(3)−Gd(2)	96.13(10)		

spheres. The third type of complexes was formed when the same reactions were carried out with at least 2 equiv of sodium acetate as a base. Monocationic trinuclear complexes ($[Ln_3L_2(X)_n(CH_3OH)]^+$, where X = bridging (CH_3COO^-) and bidentate ligands (NO_3^-, CH_3COO^-, ClO_4^-) and the total of n is 4) were produced in this case. They were composed of three Ln(III) ions, two L^{2-} ligands with bridging phenolate oxygen atoms, bridging (and/or bidentate) acetates, and bidentate nitrates. All complexes were characterized by IR spectroscopy (Table 1), mass spectrometry (Table 2), and elemental analyses (Table 3); in some cases, X-ray crystallography was also employed (Tables 5−10).

The $[LnL(NO_3)]$ and $[Ln_2L_2(NO_3)]NO_3$ complexes can be easily converted to $[Ln_3L_2(X)_n(CH_3OH)]Y$ complexes by adding 2−3 equiv of sodium acetate and 1 equiv of Ln(III) salt ($Ln(NO_3)_3$ or $LnCl_3$) or just by adding 1 equiv of a lanthanide acetate salt (Scheme 1). On the basis of IR spectra, mass spectra, and elemental analyses, the resulting $[Ln_3L_2(X)_n(CH_3OH)]Y$ complexes have the same formulation as those produced from the reactions of 1 equiv of Ln(III) salt, 1 equiv of ligand, and 2−3 equiv of sodium acetate, as summarized in Table 4. The conversion to $[Ln_3L_2(X)_n(CH_3OH)]Y$ complexes is only successful when the acetate anion is present. Other potentially bridging anions (nitrate and perchlorate) have been used in attempts to construct $[Ln_3L_2(X)_n(CH_3OH)]Y$ complexes from $[LnL(NO_3)]$ or $[Ln_2L_2(NO_3)]NO_3$; however, these reactions were not successful. When $Ln(NO_3)_3$ and 2 equiv of sodium acetate were used in this conversion, nitrate was the counteranion of the complex cation (i.e., Y = NO_3). If $LnCl_3$ was used instead of the nitrate salt, the counteranion of the complex cation was chloride (Y = Cl). If a lanthanide acetate salt was utilized, the counteranion of the product was nitrate (Y = NO_3). The

Table 9. Selected Bond Lengths (Å) and Bond Angles (deg) in the Cation of $[Gd_3(L3)_2(CH_3COO)_4(CH_3OH)]ClO_4 \cdot 0.5CH_3OH$

Gd(1)−O(1)	2.424(5)	Gd(2)−O(6)	2.347(5)
Gd(1)−O(2)	2.450(5)	Gd(2)−O(9)	2.735(5)
Gd(1)−O(5)	2.336(5)	Gd(2)−O(10)	2.441(5)
Gd(1)−O(7)	2.503(6)	Gd(2)−O(11)	2.476(5)
Gd(1)−O(8)	2.487(5)	Gd(3)−O(3)	2.364(5)
Gd(1)−N(1)	2.643(6)	Gd(3)−O(4)	2.447(5)
Gd(1)−N(2)	2.659(7)	Gd(3)−O(9)	2.432(5)
Gd(1)−N(3)	2.577(7)	Gd(3)−O(12)	2.471(5)
Gd(1)−N(4)	2.593(6)	Gd(3)−O(13)	2.500(5)
Gd(2)−O(1)	2.350(4)	Gd(3)−N(5)	2.727(6)
Gd(2)−O(2)	2.342(5)	Gd(3)−N(6)	2.598(6)
Gd(2)−O(3)	2.413(5)	Gd(3)−N(7)	2.557(6)
Gd(2)−O(4)	2.371(5)	Gd(3)−N(8)	2.553(6)
O(1)−Gd(1)−O(2)	64.39(15)	O(3)−Gd(2)−O(6)	145.9(2)
O(1)−Gd(1)−O(5)	81.5(2)	O(3)−Gd(2)−O(9)	63.3(2)
O(1)−Gd(1)−O(7)	138.2(2)	O(3)−Gd(2)−O(10)	79.0(2)
O(1)−Gd(1)−O(8)	141.4(2)	O(3)−Gd(2)−O(11)	129.8(2)
O(1)−Gd(1)−N(1)	74.3(2)	O(4)−Gd(2)−O(6)	86.8(2)
O(1)−Gd(1)−N(2)	101.9(2)	O(4)−Gd(2)−O(9)	68.3(2)
O(1)−Gd(1)−N(3)	77.6(2)	O(4)−Gd(2)−O(10)	118.4(2)
O(1)−Gd(1)−N(4)	144.6(2)	O(4)−Gd(2)−O(11)	88.1(2)
O(2)−Gd(1)−O(5)	75.1(2)	O(6)−Gd(2)−O(9)	130.6(2)
O(2)−Gd(1)−O(7)	131.2(2)	O(6)−Gd(2)−O(10)	135.0(2)
O(2)−Gd(1)−O(8)	145.7(2)	O(6)−Gd(2)−O(11)	70.6(2)
O(2)−Gd(1)−N(1)	114.7(2)	O(9)−Gd(2)−O(10)	50.2(2)
O(2)−Gd(1)−N(2)	73.1(2)	O(9)−Gd(2)−O(11)	66.8(2)
O(2)−Gd(1)−N(3)	138.6(2)	O(10)−Gd(2)−O(11)	73.5(2)
O(2)−Gd(1)−N(4)	80.2(2)	O(3)−Gd(3)−O(4)	68.9(2)
O(5)−Gd(1)−O(7)	69.9(2)	O(3)−Gd(3)−O(9)	69.0(2)
O(5)−Gd(1)−O(8)	121.9(2)	O(3)−Gd(3)−O(12)	145.4(2)
O(5)−Gd(1)−N(1)	145.0(2)	O(3)−Gd(3)−O(13)	126.5(2)
O(5)−Gd(1)−N(2)	142.4(2)	O(3)−Gd(3)−N(5)	72.0(2)
O(5)−Gd(1)−N(3)	84.0(2)	O(3)−Gd(3)−N(6)	117.7(2)
O(5)−Gd(1)−N(4)	90.9(2)	O(3)−Gd(3)−N(7)	74.6(2)
O(7)−Gd(1)−O(8)	52.1(2)	O(3)−Gd(3)−N(8)	138.6(2)
O(7)−Gd(1)−N(1)	113.5(2)	O(4)−Gd(3)−O(9)	72.5(2)
O(7)−Gd(1)−N(2)	119.4(2)	O(4)−Gd(3)−O(12)	142.7(2)
O(7)−Gd(1)−N(3)	69.8(2)	O(4)−Gd(3)−O(13)	129.2(2)
O(7)−Gd(1)−N(4)	67.7(2)	O(4)−Gd(3)−N(5)	104.3(2)
O(8)−Gd(1)−N(1)	69.9(2)	O(4)−Gd(3)−N(6)	77.8(2)
O(8)−Gd(1)−N(2)	78.1(2)	O(4)−Gd(3)−N(7)	143.3(2)
O(8)−Gd(1)−N(3)	75.4(2)	O(4)−Gd(3)−N(8)	72.2(2)
O(8)−Gd(1)−N(4)	70.8(2)	O(9)−Gd(3)−O(12)	124.7(2)
N(1)−Gd(1)−N(2)	68.7(2)	O(9)−Gd(3)−O(13)	71.6(2)
N(1)−Gd(1)−N(3)	66.5(2)	O(9)−Gd(3)−N(5)	139.1(2)
N(1)−Gd(1)−N(4)	123.3(2)	O(9)−Gd(3)−N(6)	144.3(2)
N(2)−Gd(1)−N(3)	133.5(2)	O(9)−Gd(3)−N(7)	91.7(2)
N(2)−Gd(1)−N(4)	64.5(2)	O(9)−Gd(3)−N(8)	86.6(2)
N(3)−Gd(1)−N(4)	136.2(2)	O(12)−Gd(3)−O(13)	53.1(2)
O(1)−Gd(2)−O(2)	67.2(2)	O(12)−Gd(3)−N(5)	83.2(2)
O(1)−Gd(2)−O(3)	81.4(2)	O(12)−Gd(3)−N(6)	71.5(2)
O(1)−Gd(2)−O(4)	99.4(2)	O(12)−Gd(3)−N(7)	73.5(2)
O(1)−Gd(2)−O(6)	78.8(2)	O(12)−Gd(3)−N(8)	76.0(2)
O(1)−Gd(2)−O(9)	144.7(2)	O(13)−Gd(3)−N(5)	126.3(2)
O(1)−Gd(2)−O(10)	126.7(2)	O(13)−Gd(3)−N(6)	115.5(2)
O(1)−Gd(2)−O(11)	148.0(2)	O(13)−Gd(3)−N(7)	71.9(2)
O(2)−Gd(2)−O(3)	113.7(2)	O(13)−Gd(3)−N(8)	70.9(2)
O(2)−Gd(2)−O(4)	164.8(2)	N(5)−Gd(3)−N(6)	67.3(2)
O(2)−Gd(2)−O(6)	83.6(2)	N(5)−Gd(3)−N(7)	66.3(2)
O(2)−Gd(2)−O(9)	126.7(2)	N(5)−Gd(3)−N(8)	132.3(2)
O(2)−Gd(2)−O(10)	76.5(2)	N(6)−Gd(3)−N(7)	123.9(2)
O(2)−Gd(2)−O(11)	99.7(2)	N(6)−Gd(3)−N(8)	65.5(2)
O(3)−Gd(2)−O(4)	69.3(2)	N(7)−Gd(3)−N(8)	141.3(2)
Gd(1)−O(1)−Gd(2)	111.9(2)	Gd(2)−O(3)−Gd(3)	102.5(2)
Gd(1)−O(2)−Gd(2)	111.3(2)	Gd(2)−O(4)−Gd(3)	101.3(2)

Table 10. Selected Bond Lengths (Å) and Bond Angles (deg) in the Cation of $[Sm_3(L1)_2(CH_3COO)_2(NO_3)_2(CH_3OH)]NO_3 \cdot CH_3OH \cdot 3.65H_2O$

Sm(1)−O(1)	2.385(4)	Sm(2)−O(6)	2.337(4)
Sm(1)−O(2)	2.406(3)	Sm(2)−O(10)	2.469(4)
Sm(1)−O(5)	2.361(4)	Sm(2)−O(12)	2.489(4)
Sm(1)−O(7)	2.580(4)	Sm(3)−O(3)	2.353(4)
Sm(1)−O(8)	2.569(4)	Sm(3)−O(4)	2.411(4)
Sm(1)−N(1)	2.697(4)	Sm(3)−O(11)	2.404(4)
Sm(1)−N(2)	2.626(4)	Sm(3)−O(13)	2.525(4)
Sm(1)−N(3)	2.585(5)	Sm(3)−O(14)	2.543(4)
Sm(1)−N(4)	2.540(5)	Sm(3)−N(5)	2.715(4)
Sm(2)−O(1)	2.365(4)	Sm(3)−N(6)	2.609(4)
Sm(2)−O(2)	2.377(4)	Sm(3)−N(7)	2.616(4)
Sm(2)−O(3)	2.377(4)	Sm(3)−N(8)	2.552(4)
Sm(2)−O(4)	2.403(4)		
O(1)−Sm(1)−O(2)	65.60(12)	O(3)−Sm(2)−O(4)	69.14(11)
O(1)−Sm(1)−O(5)	78.75(13)	O(3)−Sm(2)−O(6)	139.48(13)
O(1)−Sm(1)−O(7)	137.51(12)	O(3)−Sm(2)−O(10)	79.29(13)
O(1)−Sm(1)−O(8)	148.89(13)	O(3)−Sm(2)−O(12)	140.24(13)
O(1)−Sm(1)−N(1)	73.69(13)	O(4)−Sm(2)−O(6)	83.48(13)
O(1)−Sm(1)−N(2)	111.07(13)	O(4)−Sm(2)−O(10)	114.14(13)
O(1)−Sm(1)−N(3)	83.69(14)	O(4)−Sm(2)−O(12)	92.54(13)
O(1)−Sm(1)−N(4)	136.92(13)	O(6)−Sm(2)−O(10)	140.64(14)
O(2)−Sm(1)−O(5)	86.42(12)	O(6)−Sm(2)−O(12)	67.14(13)
O(2)−Sm(1)−O(7)	131.59(12)	O(10)−Sm(2)−O(12)	76.77(13)
O(2)−Sm(1)−O(8)	138.25(12)	O(3)−Sm(3)−O(4)	69.38(11)
O(2)−Sm(1)−N(1)	108.61(13)	O(3)−Sm(3)−O(11)	70.86(12)
O(2)−Sm(1)−N(2)	75.71(13)	O(3)−Sm(3)−O(13)	146.48(12)
O(2)−Sm(1)−N(3)	148.74(14)	O(3)−Sm(3)−O(14)	126.80(12)
O(2)−Sm(1)−N(4)	72.57(13)	O(3)−Sm(3)−N(5)	74.03(13)
O(5)−Sm(1)−O(7)	66.32(13)	O(3)−Sm(3)−N(6)	119.08(13)
O(5)−Sm(1)−O(8)	115.98(13)	O(3)−Sm(3)−N(7)	78.73(13)
O(5)−Sm(1)−N(1)	138.75(14)	O(3)−Sm(3)−N(8)	139.96(14)
O(5)−Sm(1)−N(2)	152.73(14)	O(4)−Sm(3)−O(11)	72.96(13)
O(5)−Sm(1)−N(3)	81.78(14)	O(4)−Sm(3)−O(13)	141.32(11)
O(5)−Sm(1)−N(4)	89.11(14)	O(4)−Sm(3)−O(14)	130.99(12)
O(7)−Sm(1)−O(8)	49.84(12)	O(4)−Sm(3)−N(5)	105.29(13)
O(7)−Sm(1)−N(1)	118.36(13)	O(4)−Sm(3)−N(6)	76.57(14)
O(7)−Sm(1)−N(2)	111.04(14)	O(4)−Sm(3)−N(7)	148.10(13)
O(7)−Sm(1)−N(3)	68.55(14)	O(4)−Sm(3)−N(8)	74.24(13)
O(7)−Sm(1)−N(4)	68.03(13)	O(11)−Sm(3)−O(13)	122.89(13)
O(8)−Sm(1)−N(1)	78.29(14)	O(11)−Sm(3)−O(14)	71.95(14)
O(8)−Sm(1)−N(2)	69.12(13)	O(11)−Sm(3)−N(5)	142.95(13)
O(8)−Sm(1)−N(3)	72.41(15)	O(11)−Sm(3)−N(6)	141.36(14)
O(8)−Sm(1)−N(4)	73.08(14)	O(11)−Sm(3)−N(7)	96.78(14)
N(1)−Sm(1)−N(2)	67.71(14)	O(11)−Sm(3)−N(8)	83.13(14)
N(1)−Sm(1)−N(3)	65.37(14)	O(13)−Sm(3)−O(14)	51.12(12)
N(1)−Sm(1)−N(4)	131.75(14)	O(13)−Sm(3)−N(5)	82.31(13)
N(2)−Sm(1)−N(3)	123.66(14)	O(13)−Sm(3)−N(6)	71.25(13)
N(2)−Sm(1)−N(4)	66.11(14)	O(13)−Sm(3)−N(7)	69.73(13)
N(3)−Sm(1)−N(4)	135.63(15)	O(13)−Sm(3)−N(8)	73.42(14)
O(1)−Sm(2)−O(2)	66.37(12)	O(14)−Sm(3)−N(5)	123.31(13)
O(1)−Sm(2)−O(3)	80.07(12)	O(14)−Sm(3)−N(6)	113.81(14)
O(1)−Sm(2)−O(4)	101.75(12)	O(14)−Sm(3)−N(7)	69.39(13)
O(1)−Sm(2)−O(6)	76.90(12)	O(14)−Sm(3)−N(8)	68.58(13)
O(1)−Sm(2)−O(10)	128.08(12)	N(5)−Sm(3)−N(6)	68.30(13)
O(1)−Sm(2)−O(12)	139.40(13)	N(5)−Sm(3)−N(7)	64.66(13)
O(2)−Sm(2)−O(3)	113.15(12)	N(5)−Sm(3)−N(8)	132.98(14)
O(2)−Sm(2)−O(4)	166.43(12)	N(6)−Sm(3)−N(7)	121.40(14)
O(2)−Sm(2)−O(6)	87.25(13)	N(6)−Sm(3)−N(8)	65.98(14)
O(2)−Sm(2)−O(10)	79.22(13)	N(7)−Sm(3)−N(8)	135.69(14)
O(2)−Sm(2)−O(12)	92.96(13)		
Sm(1)−O(1)−Sm(2)	110.79(15)	Sm(2)−O(3)−Sm(3)	104.08(12)
Sm(1)−O(2)−Sm(2)	109.64(14)	Sm(2)−O(4)−Sm(3)	101.55(11)

mechanism of this interconversion has not yet been studied; it possibly, however, involves rearrangement of each unit instead of simply the insertion of the middle Ln unit.

Selected IR stretching frequencies of all complexes are listed in Table 1. The $[LnL(NO_3)]$ complexes show stretching frequencies typical of bidentate nitrates (1480 and 1300 cm^{-1}. However, they lack the strong stretching bands of free (non-coordinated) anionic nitrate (Figure 1); instead, they exhibit weaker bands due to the ligands around 1385 cm^{-1}. Because of the overlapping ligand and free nitrate bands, IR spectra alone are not an adequate tool to indicate the absence of free nitrates in the mononuclear complexes. The $[Ln_2L_2(NO_3)]NO_3$ complexes show both bidentate nitrate bands (1480 and 1290 cm^{-1}) and a free anionic nitrate band at 1384 cm^{-1} (Figure 1). Both the former and the latter are consistent with the literature values reported for $[La(NO_3)_3(phen)_2]$.[30]

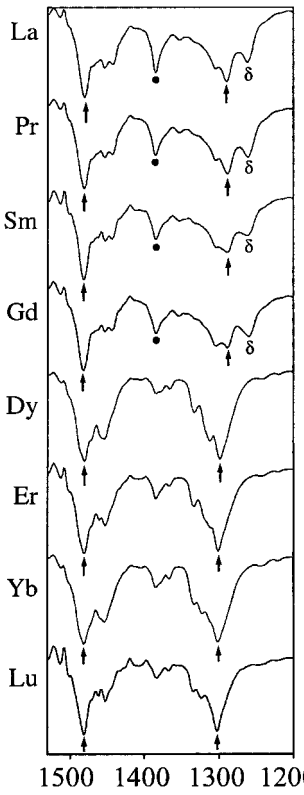

Figure 1. IR bands (1520−1200 cm^{-1}) of all mononuclear $[LnL(NO_3)]$ (Ln = Dy−Lu) and dinuclear $[Ln_2L_2(NO_3)]NO_3$ (Ln = La−Gd) complexes: ↑, bidentate nitrate stretching bands; δ, C−O deformation bands of bridging phenolates; •, free (uncoordinated) nitrate stretching bands.

Another significant difference between the $[LnL(NO_3)]$ and $[Ln_2L_2(NO_3)]NO_3$ complexes is the presence of a band at 1260 cm^{-1} in the spectra of the latter (Figure 1), possibly a deformation band of a bridging phenolate group. A characteristically strong deformation band of the phenolato ligand is found in the spectra of phenoxide erbium complexes, where it appears at 1270 cm^{-1}.[31] The deformation band of nonbridging phenolates in the $[LnL(NO_3)]$ complexes overlaps with the lower frequency band of the bridging nitrate, resulting in a strong broad band around 1300 cm^{-1}.

The trinuclear complexes ($[Ln_3L_2(X)_n(CH_3OH)]Y$) have more complicated infrared stretching vibrations because of the presence of bridging phenolates, free anionic nitrate, free hexafluorophosphate, or free perchlorate counteranions (Y), bridging acetates, and bidentate acetates or nitrates in some cases. The nitrate bands (bidentate and anionic) appear at the same frequencies as in the spectra of the $[LnL(NO_3)]$ and $[Ln_2L_2(NO_3)]NO_3$ complexes. The deformation bands of bridging phenolates are also as observed for the latter complexes. In the

(30) Hart, F. A.; Laming, F. P. *J. Inorg. Nucl. Chem.* **1965**, *27*, 1605 and references therein.
(31) Mehrotra, R. C.; Batwara, J. M. *Inorg. Chem.* **1970**, *9*, 2505.

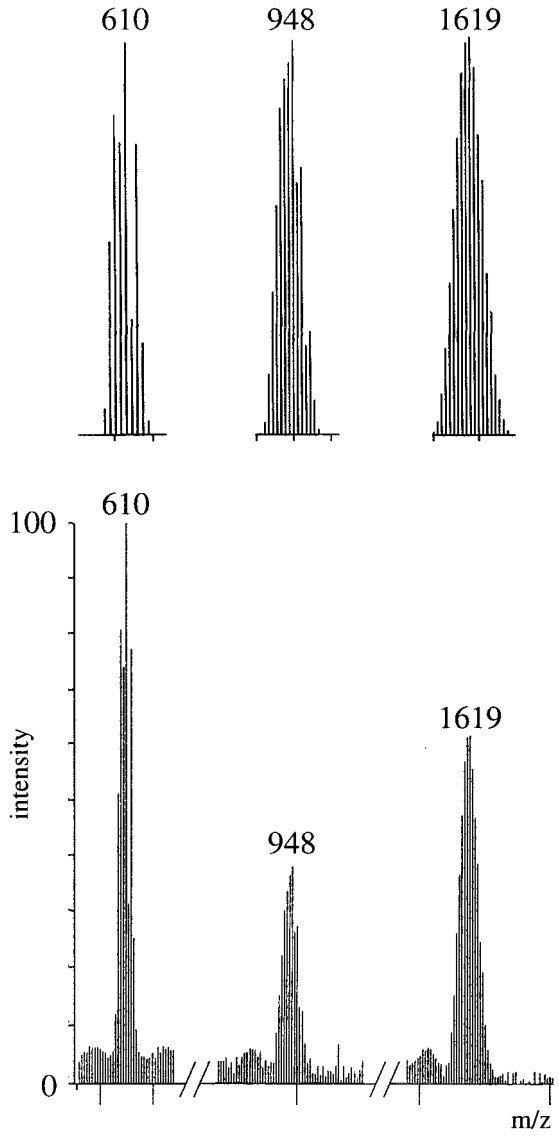

Figure 2. Experimental (lower) and simulated (upper) isotopic patterns for major peaks in the mass spectrum of trinuclear $[Gd_3(L1)_2(CH_3COO)_2(NO_3)_2(CH_3OH)]NO_3$.

cases where acetate is present as a bridging ligand, ν_{COO^-} appears around 1560 and 1412 cm^{-1}, a frequency difference of approximately 150 cm^{-1}. In other cases where acetate is also present as a bidentate chelating ligand, ν_{COO^-} appears around 1530−1550 and 1450 cm^{-1}. The difference between these two bands (∼100 cm^{-1}) is smaller than that for a bridging acetate, consistent with the literature.[32]

The LSIMS spectra of all complexes were obtained in a thioglycerol matrix in the positive-ion-detection mode. The complete results are presented in Table 2. For the $[LnL(NO_3)]$ complexes, $[LnL]^+$ parent peaks are observed, as they are for the $[Ln_2L_2(NO_3)]NO_3$ complexes. In addition to $[LnL]^+$ peaks, $[Ln_2L_2(NO_3)]^+$ peaks are present in the spectra of the latter. These peaks, along with the presence of C−O bridging phenolate deformation bands in the IR spectra (vide supra), were used to confirm the dinuclearity of these complexes. Generally, the spectra of the $[Ln_3L_2(X)_n(CH_3OH)]Y$ complexes show parent peaks of intact monocationic $[Ln_3L_2(CH_3COO)_2(NO_3)_2]^+$ and of $[Ln_2L(CH_3COO)_2(NO_3)]^+$ and $[LnL]^+$ fragments (Figure 2).

(32) Deacon, G. B.; Phillips, R. J. *Coord. Chem. Rev.* **1980**, *33*, 227.

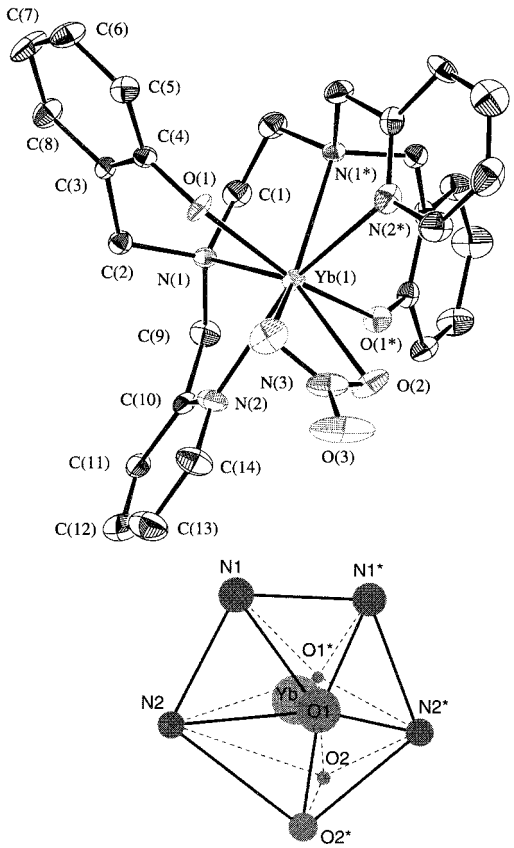

Figure 3. ORTEP diagram of $[Yb(L1)(NO_3)]$ and a scheme of the coordination geometry around Yb(III), shown with the same numbering as the crystallographic numbering. Thermal ellipsoids for the non-hydrogen atoms are drawn at the 33% probability level.

The detection of intact high molecular weight parent peaks in the mass spectra strongly suggests the stability of these trinuclear molecules.

The magnetic moments of some complexes were measured at room temperature (Table 3). They are similar to the calculated μ_{eff} values (calculated on the basis of J). In general, the Ln(III) ions are magnetically dilute (not interacting); a very weak exchange ($-J = 0.045$ cm^{-1}) was found in an encapsulated dimer of an amino phenolato Gd(III) complex.[33]

Selected crystallographic data for all five structures are presented in Table 5. The X-ray structural analysis (Figure 3) shows that mononuclear $[Yb(L1)(NO_3)]$ consists of one Yb atom, one hexadentate $L1^{2-}$ ligand, and one bidentate nitrate. This molecule has a C_2 axis, and the coordination number of Yb(III) is 8. The coordination geometry around Yb can be best described as a distorted dodecahedron (Figure 3). The hexadentate $L1^{2-}$ ligand forms a "cap" around the Yb(III) center with an O(1)−Yb−O(1*) angle of 156.3° and an N(2)−Yb−N(2*) angle of 155.5°. Complexes of Ga(III) and In(III) with hexadentate $L2^{2-}$ exhibit octahedral geometry around the metal centers, with a greater degree of distortion in the latter.[26] The cavity around hexadentate $L1^{2-}$ is too small to completely encapsulate a larger Yb(III) ion;[34] thus, along with a bidentate nitrate to satisfy a higher coordination number of Yb(III), $L1^{2-}$ forms a dodecahedral geometry around the central metal ion. Kepert[35−37] predicted that the dodecahedral geometry should

(33) Liu, S.; Gelmini, L.; Rettig, S. J.; Thompson, R. C.; Orvig, C. *J. Am. Chem. Soc.* **1992**, *114*, 6081.
(34) Shannon, R. D. *Acta Crystallogr., Sect. A* **1976**, *32*, 751.
(35) Kepert, D. L. *J. Chem. Soc.* **1965**, 4736.
(36) Blight, D. G.; Kepert, D. L. *Theor. Chim. Acta* **1968**, *11*, 51.

be significantly stabilized relative to the square antiprismatic geometry for small "bite" ligands, such as bidentate nitrate.

Selected bond lengths and bond angles are presented in Table 6. The average Yb−N bond length is 2.506 Å, similar to those of an eight-coordinate Yb complex (Yb−N(av) 2.52 Å)[38] and a seven-coordinate Yb amine phenolate complex (Yb−N(av) 2.497 Å).[39] The Yb−O(phenolate) bond length is 2.163(4) Å, which is similar to that reported by Yang et al. (Yb−O(av) 2.158 Å).[39] The Yb−O(nitrate) (Yb(1)−O(2) = 2.432 Å) bond length is similar to that of ten-coordinated $K_2[Er(NO_3)_5]$, which has an average Yb−O(nitrate) value of 2.431 Å.[40] The O(2)−N(3)−O(2*) angle is 116.8°, smaller than that in unbound nitrate (120°). In fact, this is true for all the bidentate nitrates in all the structures reported herein. This is consistent with O−N−O angles of the bidentate nitrates in trinitrato[1,2-bis(pyridine-2-carbaldimino)ethane]gadolinium(III), ranging from 115.1 to 117.4°.[41]

The structural analysis of dinuclear $[Pr_2(L1)_2(NO_3)(H_2O)]NO_3$ (Figure 4) shows the presence of two praseodymium atoms (Pr(1) and Pr(2)), one hexadentate ligand ($L1^{2-}$) with only terminal phenolate oxygen atoms (O(1) and (O(2)), another $L1^{2-}$ with two phenolate oxygen atoms (O(3) and O(4)) bridging between Pr(1) and Pr(2), and one bidentate nitrate bound at Pr-(2). Thus, the coordination numbers of Pr(1) and Pr(2) are 8 and 9, respectively. The geometry around Pr(1) is best described as a distorted cube, while the geometry around Pr(2) is closest to a monocapped square antiprism, with coplanar O(3), O(4), N(5), and N(6) forming one square face and coplanar O(6), O(8), N(7), and N(8) forming the other square face, with O(5) as a cap (Figure 4). The cubic geometry around Pr(1) is one of a few rare examples of cubic geometry in Ln(III) complexes.[18,42−46] A theoretical molecular orbital analysis by Hoffmann and co-workers[42] determined that the cubic geometry is less stable than the more common dodecahedron, square antiprism, or bicapped trigonal prism due to electronic and steric effects. The monocapped square antiprismatic geometry around Pr(2) is a common coordination geometry for complexes with coordination number of 9. In fact, all structures with coordination number 9 reported herein have the same type of geometry, with the exception of the geometry around Gd(2) in dinuclear $[Gd_2(L1)_2(NO_3)]^+$ (vide infra).

Selected bond lengths and bond angles are listed in Table 7. The average bond length of terminal oxygen atoms to Pr(1) (Pr-(1)−O(1) and Pr(1)−O(2)) is 2.335 Å. This value is similar to a six-coordinate Pr−O(terminal phenolate) average bond length of 2.341 Å.[47] Since the bridging oxygen atoms (O(3) and O(4)) form two strong Pr−O bonds, their basicity should be lowered relative to that of singly bonded O atoms; the bridging Pr−O distance (average of 2.434 Å) is 0.08 Å lower than the Pr−O(terminal) distance, as expected. The angles at the phenolate oxygen bridgeheads are 113.71(7)° (O(3)) and 109.31(7)° (O(4)).

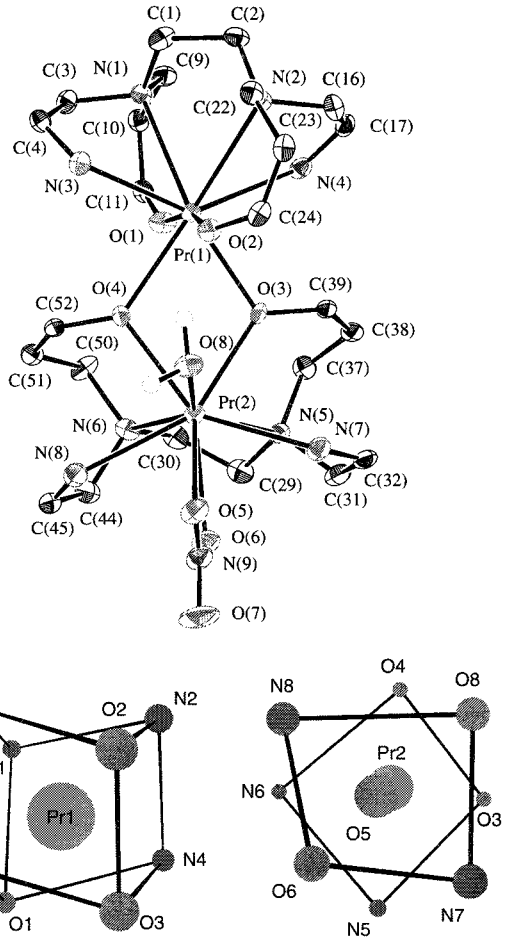

Figure 4. ORTEP diagram of the $[Pr_2(L1)_2(NO_3)(H_2O)]^+$ cation in $[Pr_2(L1)_2(NO_3)(H_2O)]NO_3 \cdot CH_3OH$ and a scheme of the coordination geometries around each Pr(III) center, shown with the same numbering as the crystallographic numbering. Thermal ellipsoids for the non-hydrogen atoms are drawn at the 33% probability level, and some of the phenolate and pyridyl ring atoms have been omitted for clarity.

The distance between the two metal centers (Pr(1)···Pr(2)) is 4.022 Å. The bond length of Pr−O(nitrate) is 2.588 Å, slightly lower than that found in a phenolate Schiff base complex of praseodymium.[48] The Pr−O(water) bond length (2.448 Å) is similar to that of Kahwa et al. (2.535 Å).[49] The average Pr−N bond length is 2.706 Å, shorter than the Pr−N distance expected on the basis of Gd−N bond lengths (2.695 Å average)[47] after correcting for the difference of ionic radii between the two metal ions.[34]

The X-ray crystal structure of $[Gd_2(L1)_2(NO_3)]NO_3$ (Figure 5) shows a dinuclear $[Gd_2L_2(NO_3)]^+$ unit different from its Pr congener in that three phenolate oxygen atoms bridge the two Gd atoms. Gd(1) is coordinated by hexadentate $L1^{2-}$, in which there is one bridging phenolate oxygen (O(2)), and also by two bridging phenolate oxygen atoms from the second ligand (O(3) and O(4)); thus, the coordination number of Gd(1) is 8. Gd(2) is coordinated to the bridging phenolate oxygen O(2), the second hexadentate ligand with its two bridging phenolate oxygen atoms, and one bidentate nitrate. The coordination number of Gd(2) is 9. Figure 5 also shows the coordination polyhedron around each Gd(III) ion. The coordination geometry around Gd-(1) is best described as a distorted square antiprism which

(37) Blight, D. G.; Kepert, D. L. *Inorg. Chem.* **1972**, *11*, 1556.
(38) Baraniak, E.; Bruce, R. S. L.; Freeman, H. C.; Hair, N. J.; James, J. *Inorg. Chem.* **1976**, *15*, 2226.
(39) Yang, L.-W.; Liu, S.; Wong, E.; Rettig, S. J.; Orvig, C. *Inorg. Chem.* **1995**, *34*, 2164.
(40) Sherry, E. G. *J. Inorg. Nucl. Chem.* **1978**, *40*, 257.
(41) Smith, G. D.; Caughlan, C. N.; Mahzar-Ul-Haque; Hart, F. A. *Inorg. Chem.* **1973**, *12*, 2654.
(42) Burdett, J. K.; Hoffmann, R.; Fay, R. C. *Inorg. Chem.* **1978**, *17*, 2553.
(43) Muetterties, E. L.; Wright, C. H. *Q. Rev., Chem. Soc.* **1967**, *21*, 109.
(44) Lippard, S. J. *Prog. Inorg. Chem.* **1967**, *8*, 109.
(45) Sinha, S. P. *Struct. Bonding* **1976**, *25*, 69.
(46) Al-Karaghouli, A. R.; Day, R. O.; Wood, J. S. *Inorg. Chem.* **1978**, *17*, 3702.
(47) Liu, S.; Yang, L.-W.; Rettig, S. J.; Orvig, C. *Inorg. Chem.* **1993**, *32*, 2773.
(48) Kahwa, I. A.; Fronczek, F. R.; Selbin, J. *Inorg. Chim. Acta* **1987**, *126*, 227.
(49) Kahwa, I. A.; Selbin, J.; O'Connor, C. J.; Foise, J. W.; McPherson, G. L. *Inorg. Chim. Acta* **1988**, *148*, 265.

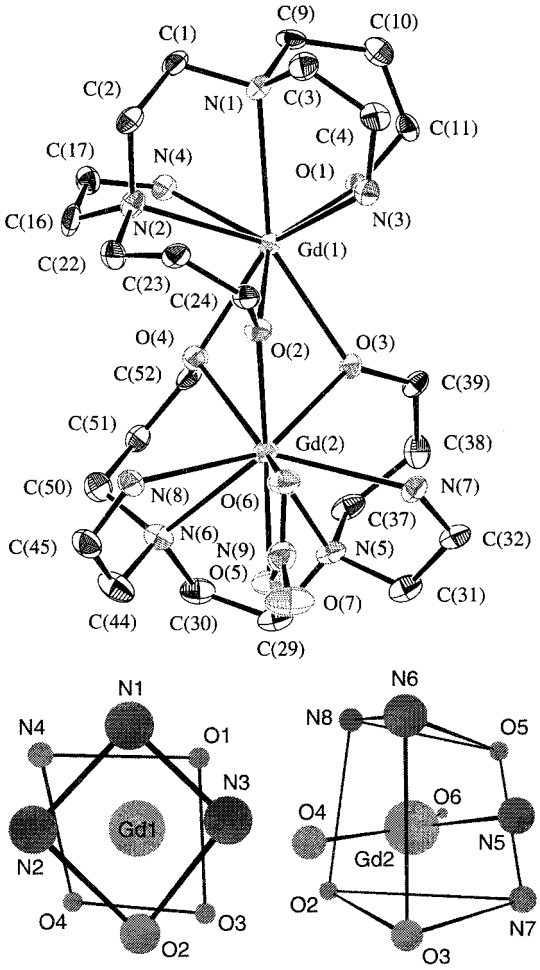

Figure 5. ORTEP diagram of the $[Gd_2(L1)_2(NO_3)]^+$ cation in $[Gd_2(L1)_2(NO_3)]NO_3{\cdot}CH_3OH{\cdot}3H_2O$ and a scheme of the coordination geometries around each Gd(III) center, shown with the same numbering as the crystallographic numbering. Thermal ellipsoids for the non-hydrogen atoms are drawn at the 33% probability level, and some of the phenolate and pyridyl ring atoms have been omitted for clarity.

consists of coplanar N(1), N(2), N(3), and O(2) atoms and a second coplanar set of N(4), O(1), O(3), and O(4) atoms. The geometry around Gd(2) can be described as a distorted tricapped trigonal prism with O(4), O(6), and N(5) as the capping atoms. Square antiprismatic geometry is also well-known among eight-coordinate structures.[42] The geometry around Gd(1), with three bridging phenolate oxygen atoms and with an ionic radius between those of Yb(III) and Pr(III),[34] seems to be the midpoint between an eight-coordinate dodecahedron $[Yb(L1)(NO_3)]$ and the cubic geometry around Pr(1) in $[Pr_2(L1)_2(NO_3)(H_2O)]^+$ (vide supra). The tricapped trigonal prism found around Gd(2) is common among nine-coordinate structures.[50]

Selected bond angles and bond lengths are summarized in Table 8. The Gd−N distances have an average value of 2.636 Å, consistent with that of an eight-coordinated dimeric amine phenol (N_4O_3) complex of Gd(III) (2.69 Å)[47] and longer than that of a Gd(III) complex with an acylic Schiff base ligand (2.349 Å).[15] The Gd−O(terminal phenolate) (Gd(1)−O(1)) distance is 2.230 Å, similar to those reported by Liu et al. (2.253 Å) and Howell et al. (2.207 Å). This Gd−O(terminal phenolate) distance is again shorter than the average Gd−O(bridging phenolate) distance of 2.412 Å in $[Gd_2(L1)_2(NO_3)]^+$, consistent with the literature.[15,47] The difference of 0.18 Å between the former and the latter is slightly larger than those of a dimeric amine phenol (N_4O_3) complex of Gd (0.13 Å)[33] and of a dimeric Gd−acyclic Schiff base complex (0.14 Å).[15] The angles at the phenolate oxygen bridgeheads are 100.03° (Gd(1)−O(2)−Gd(2)), 96.13° (Gd(1)−O(3)−Gd(2)), and 97.28° (Gd(1)−O(4)−Gd(2)). Smaller angles at the phenolate oxygen bridgeheads compared to those of Liu et al. (113.12°) and Howell et al. (108.7°)[15] and the steric hindrance related the three bridging phenolate oxygen atoms result in a closer distance between the two gadolinium centers and longer Gd−O(bridging phenolate) bond lengths. The Gd(1)···Gd(2) separation in $[Gd_2(L1)_2(NO_3)]^+$ is 3.636 Å, shorter than the 3.984 Å distance in $[Gd_2(N_4O_3)_2]$[47] and the 3.81 Å value reported by Howell et al.[15] To our knowledge, this is the first characterized dinuclear Ln(III) structure with three phenolate oxygen bridges between the two metal ions. The Gd−O(nitrate) bond lengths (Gd(2)−O(5) 2.481 Å and Gd(2)−O(6) 2.507 Å) are consistent with that of another eight-coordinate dimeric gadolinium imino phenolate complex reported by Howell et al. (2.494 Å).[15]

The X-ray structural analysis of trinuclear $[Gd_3(L3)_2(CH_3COO)_4(CH_3OH)]ClO_4$ shows the presence of three Gd(III) ions, two $L3^{2-}$ ligands with all phenolate oxygen atoms forming bridges, one methanol molecule, two bidentate acetates, one acetate bridging in the classical μ_2-η^1:η^1 fashion, and another (tridentate) acetate bridging in the less common μ_2-η^2:η^1 fashion, where one of the acetate oxygen atoms (O(9)) is bound to two Gd(III) centers (Gd(2) and Gd(3)) (Figure 6). The geometry around nine-coordinated Gd(1) is best described as a distorted monocapped square antiprism with O(1), O(2), N(1), and N(2) forming one square face and N(3), N(4), O(5), and O(8) forming the other square face, with O(7) as a cap (Figure 6). Gd(2) has eight oxygen atoms in its coordination sphere which can be described as a distorted bicapped trigonal prism of which O(6) and O(9) are the capping atoms (Figure 6). Gd(3) has a coordination number of 9, and its geometry can be described as a distorted monocapped square antiprism (Figure 6). Atoms O(3), O(4), N(5), and N(6) form a square face as do N(7), N(8), O(9), and O(12), with O(13) as a capping atom. Thus, the coordination environment around Gd(3) is exactly the same as that around Gd(1). Along with the dodecahedron and the square antiprism, the bicapped trigonal prism is also quite common in eight-coordinate structures. Comparison between the geometries around Gd(2) in the trinuclear Gd(III) complex and Sm(2) in the trinuclear Sm(III) congener (vide infra) shows that the second capping atom (O(9)) in the former is in just the right position and at just the right distance for coordination with Gd(2). Meanwhile, such a bond is absent in the trinuclear Sm(III) complex due to the larger ionic radius of Sm(III).[34] This is consistent with the literature stating that the bicapped trigonal prism is the halfway point between a seven-coordinate monocapped trigonal prism and a nine-coordinate tricapped trigonal prism.[42]

Selected bond lengths and bond angles for the cation in $[Gd_3(L3)_2(CH_3COO)_4(CH_3OH)]ClO_4$ are summarized in Table 9. The average Gd−N bond length is 2.613 Å, similar to that of another nine-coordinate $Gd[N_6O_4]$ hexaazamacrocycle with four phenolate pendant arms (Gd−N(av) 2.63 Å).[51] The average Gd−O(bridging phenolate) distance is 2.397 Å, and the angles at the O(1), O(2), O(3), and O(4) bridgeheads are 111.9, 111.3, 102.5, and 101.3°, respectively. The Gd···Gd separations are 3.956 Å (Gd(1)···Gd(2)) and 3.726 Å (Gd(2)···Gd(3)). They are slightly shorter than the Gd···Gd separations in the Gd_2-

(50) Drew, H. G. B. *Coord. Chem. Rev.* **1977**, *24*, 179.

(51) Bligh, S. W. A.; Choi, N.; Cummins, W. J.; Evagorou, E. G.; Kelly, J. D.; McPartlin, M. *J. Chem. Soc., Dalton Trans.* **1993**, 3829.

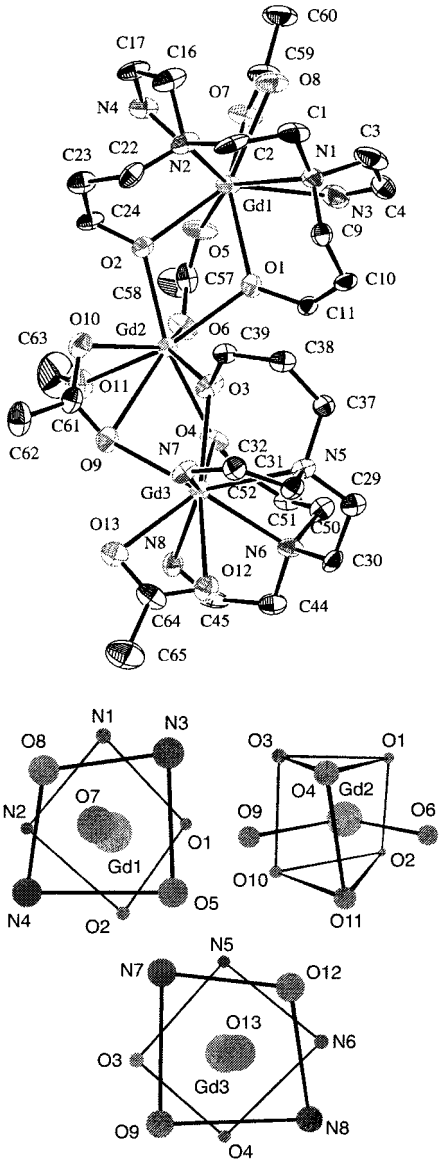

Figure 6. ORTEP diagram of the $[Gd_3(L3)_2(CH_3COO)_4(CH_3OH)]^+$ cation in $[Gd_3(L3)_2(CH_3COO)_4(CH_3OH)]ClO_4 \cdot 5CH_3OH$ and a scheme of the coordination geometries around each Gd(III) center, shown with the same numbering as the crystallographic numbering. Thermal ellipsoids for the non-hydrogen atoms are drawn at the 33% probability level, and some of the phenolate and pyridyl ring atoms have been omitted for clarity.

$[N_4O_3]_2$ dimer, which contains only phenolate oxygen bridges (3.9841 Å),[47] and in $[Gd_2(CH_3COO)_8]^{2-}$, which contains four acetate bridges (3.960 Å).[19] The Gd−O(bidentate acetate) bond lengths average 2.490 Å, and the average Gd−O(bridging acetate) distance is slightly shorter, at 2.375 Å. The tridentate bridging phenolate oxygen (O(9)) has a significantly shorter bond distance to Gd(3) (2.432 Å) compared to the Gd(2)−O(9) bond distance of 2.735 Å.

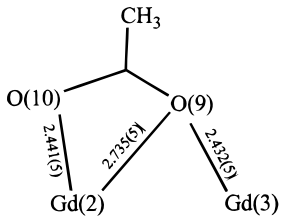

All of these Gd−O(acetate) bond lengths are consistent with those measured in $[Gd_2(CH_3COO)_8]^{2-}$.[19] Ouchi et al.[20] have reported tridentate acetate bridging of several lanthanide metal ions where the bond length to one metal ion is shorter than the one to another metal ion. The Gd−O(CH_3OH) bond length is 2.486 Å.

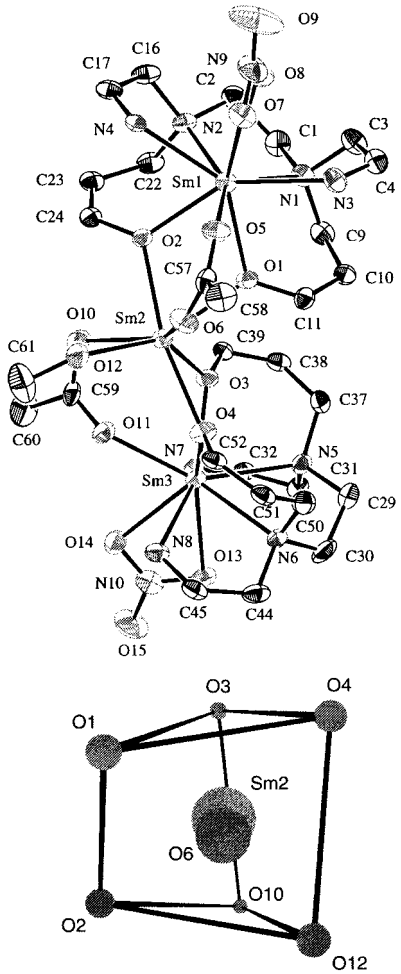

Figure 7. ORTEP diagram of the $[Sm_3(L1)_2(CH_3COO)_2(NO_3)_2(CH_3OH)]^+$ cation in $[Sm_3(L1)_2(CH_3COO)_2(NO_3)_2(CH_3OH)]NO_3 \cdot CH_3OH \cdot 3.65H_2O$ and a scheme of the coordination geometry around Sm(2), shown with the same numbering as the crystallographic numbering. Thermal ellipsoids for the non-hydrogen atoms are drawn at the 33% probability level, and some of the phenolate and pyridyl ring atoms have been omitted for clarity.

The X-ray crystal structure of $[Sm_3(L1)_2(CH_3COO)_2(NO_3)_2(CH_3OH)]NO_3$ (Figure 7) shows the presence of three Sm(III) ions, two $L1^{2-}$ ligands with all four phenolate oxygen atoms forming bridges, one methanol molecule, two bidentate nitrate groups on two Sm(III) metal centers, and two acetate groups bridging in the classical μ_2-η^1:η^1 fashion. Sm(1) is nine-coordinate with a monocapped square antiprismatic geometry. One face of the square is composed of O(1), O(2), N(1), and N(2), and the second square is composed of N(3), N(4), O(5), and O(8), with O(7) as the capping atom (as shown for Gd(1) in Figure 6). Sm(2) is coordinated to seven oxygen atoms. The geometry around this center is best described as a distorted monocapped trigonal prism with O(6) as the capping atom (Figure 7). Sm(3) has a coordination number of 9; its geometry at the metal center can be best described as a monocapped square antiprism. The faces of the squares consist of atoms O(3), O(4), N(5), and N(6) and of atoms N(7), N(8), O(11), and O(13), with O(14) capping the latter face (as shown for Gd(3) in Figure 6). The polyhedral geometries around Sm(1) and Sm(3) are

virtually identical to those around Gd(1) and Gd(3), respectively, with a different numbering system of oxygen atoms around Sm(3) due to the replacement of a bidentate nitrate with a bidentate acetate in $[Gd_3(L3)_2(CH_3COO)_4(CH_3OH)]ClO_4$. The similarities in the X-ray crystal structures of $[Gd_3(L3)_2(CH_3COO)_4(CH_3OH)]ClO_4$ and $[Sm_3(L1)_2(CH_3COO)_2(NO_3)_2(CH_3OH)]NO_3$ show that reactions using different Ln(III) starting materials, with either the bromo-substituted or the unsubstituted ligand, and 2−3 equiv of sodium acetate will produce the same $[Ln_3L_2(X)_n(CH_3OH)]^+$ complex.

Table 10 summarizes the selected bond angles and bond lengths for the cation of trinuclear $[Sm_3(L1)_2(CH_3COO)_2(NO_3)_2(CH_3OH)]NO_3$. The average Sm−N bond length is 2.618 Å, similar to that of samarium ten-coordinated with an imino pyridyl hexadentate ligand (Sm−N(av) 2.63 Å).[52] The average phenolate oxygen atom to Sm(III) bond length is 2.385 Å, similar to that in its gadolinium congener even though the ionic radius of Sm(III) is slightly larger than that of Gd(III).[34] The angles at the phenolate oxygen bridgeheads are 110.79, 109.64, 104.08, and 101.55° at O(1), O(2), O(3), and O(4), respectively. The intra-Sm(III) distances are 3.910 Å (Sm(1)···Sm(2)) and 3.729 Å (Sm(2)···Sm(3)), very similar to, if not even smaller than, the Gd···Gd distances in $[Gd_3(L3)_2(CH_3COO)_4(CH_3OH)]ClO_4$. In the trinuclear Sm(III) complex, there is only one type of acetate present, the classical μ_2-η^1:η^1 bridging acetate. The average Sm−O(bridging acetate) distance is 2.393 Å, consistent with the case of $[Gd_2(CH_3COO)_8]^{2-}$,[19] after correcting for the difference in ionic radii between the two metal ions.[34] The absence of a tridentate (μ_2-η^2:η^1) acetate is the only difference between the trinuclear Sm(III) and Gd(III) complexes. This difference may be due to the larger ionic radius of Sm(III), pushing the distance of O(11) to Sm(2) to be too large for a bond to be formed. The Sm−O(nitrate) bond lengths are also consistent with those of other Sm(III) complexes containing bidentate nitrate.[52−54] The bond length of Sm−O(MeOH) is 2.489 Å, similar to its Gd congener (vide supra).

The hexadentate ligands ($L1^{2-}$−$L3^{2-}$) reported herein are unique in their ability to accommodate different sizes of Ln(III) ions in the presence of small potentially bridging ligands, such as nitrate and acetate. Myriad types of coordination modes were discovered: the commonly known seven-coordinate monocapped trigonal prism, eight-coordinate dodecahedron, square antiprism, and bicapped trigonal prism, nine-coordinate monocapped square antiprism, and tricapped trigonal prism and a rare eight-coordinate cubic geometry.

The formation of binuclear complexes of the larger Ln(III) ions with L^{2-} was not unexpected, since ligands with phenolate oxygen atoms have been known to form bridges between two metal ions.[13,15,47] These oxygen atoms are prone to bridge as a requirement of the higher coordination numbers for Ln(III) ions. A designed mismatch between Ln(III) coordination numbers and ligand denticity can be used to create new multimetallic motifs. It was not expected that the use of acetate as a base would produce different complexes (trinuclear) that contain bridging phenolate oxygen atoms as well as bridging acetates. $Ln_2[N_4O_3]_2$[47] complexes were synthesized with either sodium hydroxide or sodium acetate as a base. As well, Caravan et al.[11] have reported the complexation of a ligand that contains two pyridyl and two acetate pendant arms on an ethylenediamine backbone (bis(2-pyridylmethyl)ethylenediamine-*N*,*N*′-diacetic acid (H_2bped)) with Ln(III) ions. The use of sodium acetate base in the reactions of Ln(III) ions with either Liu's $[N_4O_3]$[47] or Caravan's H_2bped[11] did not produce any trinuclear complexes. Since no trinuclear Ln(III) complexes were formed with amino phenolate[39,47] and amino pyridyl carboxylate[11] ligands even in the presence of acetate, the formation of trinuclear complexes with amino pyridyl phenolate ligands reported herein suggests the stability of this system. This stability is also evinced by the ease of conversion from either mononuclear or dinuclear complexes as long as the acetate anion is present (Scheme 1) and by the presence of high molecular weight trinuclear parent peaks of complexes in the mass spectra.

Conclusions

Three types of Ln(III) complexes with $L1^{2-}$, $L2^{2-}$, and $L3^{2-}$ were synthesized and characterized. The formation of each type of complex depended on the size of the Ln(III) ion and on the base used in the reaction (NaOH produced mononuclear and dinuclear complexes, while sodium acetate produced trinuclear complexes). The X-ray crystal structures of the dinuclear and trinuclear complexes showed the presence of bridging phenolate oxygen atoms in both and bridging acetate groups in the latter. The conversion from mononuclear or dinuclear to trinuclear complexes could be easily performed by adding at least 2 equiv of sodium acetate and 1 equiv of Ln(III) salt.

Acknowledgment. We gratefully acknowledge DuPont Pharmaceuticals for operating grants and the Natural Sciences and Engineering Research Council of Canada for a graduate fellowship (I.A.S.) and for operating grants. We also thank Dr. P. Wassell for the use of his magnetometer for the room-temperature studies.

Supporting Information Available: Complete tables of crystallographic data, final atomic coordinates and equivalent isotropic thermal parameters, anisotropic thermal parameters, bond lengths, bond angles, hydrogen atom coordinates, torsion angles, intermolecular contacts, bond lengths and angles involving hydrogen bonding, and least-squares planes. This material is available free of charge via the Internet at http://pubs.acs.org.

IC991170J

(52) Abid, K. K.; Fenton, D. E.; Casellato, U.; Vigato, P. A.; Graziani, R. *J. Chem. Soc., Dalton Trans.* **1984**, 351.
(53) Burns, J. H. *Inorg. Chem.* **1979**, *18*, 3044.
(54) Tomat, G.; Valle, G.; Cassol, A.; Di Bernardo, P. *Inorg. Chim. Acta* **1983**, *76*, L13.